

University of Szeged

Faculty of Pharmacy

Institute of Pharmaceutical Technology and Regulatory Affairs

Head: Prof. Dr. Ildikó Csóka Ph.D.

**Investigation of the Feasibility and Efficiency of Cyclodextrin
Complexation via Solvent-Free Co-Grinding with Different Active
Substances**

Ph.D. Thesis

Dr. Balázs Attila Kondoros, Pharm.D.

Supervisors:

Prof. Dr. Ildikó Csóka Ph.D.

and

Dr. habil Rita Ambrus Ph.D.

SZEGED

2023

PUBLICATIONS

- (1) **Kondoros, B. A.**; Jójárt-Laczkovich, O.; Berkesi, O.; Szabó-Révész, P.; Csóka, I.; Ambrus, R.; Aigner, Z. Development of Solvent-Free Co-Ground Method to Produce Terbinafine Hydrochloride Cyclodextrin Binary Systems; Structural and In Vitro Characterizations.
Pharmaceutics 2022, 14 (4), 744. <https://doi.org/10.3390/pharmaceutics14040744>.
Q1 IF = 5.4 (2022)
- (2) **Kondoros, B. A.**; Berkesi, O.; Tóth, Z.; Aigner, Z.; Ambrus, R.; Csóka, I. Cyclodextrin Complexation of Fenofibrate by Co-Grinding Method and Monitoring the Process Using Complementary Analytical Tools.
Pharmaceutics 2022, 14 (7), 1329. <https://doi.org/10.3390/pharmaceutics14071329>.
Q1 IF = 5.4 (2022)
- (3) **Kondoros, B. A.**; Kókai, D.; Burián, K.; Sorrenti, M.; Catenacci, L.; Csóka, I.; Ambrus, R. Ternary cyclodextrin systems of terbinafine hydrochloride inclusion complexes: Solventless preparation, solid-state, and in vitro characterization.
Heliyon 2023. <https://doi.org/10.1016/j.heliyon.2023.e21416>
Q1 IF = 4.0 (2023)
- (4) **Kondoros, B. A.**; Csóka, I.; Ambrus, R. Short-term stability studies of amorphous cyclodextrin complexes prepared by co-grinding.
Acta Pharmaceutica Hungarica 2023. Accepted for publication.
Q4 IF = -

PRESENTATIONS

Oral presentations

- (1) **Kondoros, B. A.**; Aigner, Z. – Physicochemical characterization and dissolution studies of terbinafine hydrochloride–cyclodextrin complexes prepared by solvent-free co-grinding. II. Symposium of Young Researchers on Pharmaceutical Technology, Biotechnology and Regulatory Science, Szeged, Jan 2020
- (2) **Kondoros, B.A.**; Laczkovich, O.; Berkesi, O.; Aigner, Z. – Analytical investigation of organic solvent-free co-grinding technique in terbinafine hydrochloride cyclodextrin complexation. Congressus Pharmaceuticus Hungaricus XVI., Debrecen, Sept 2020

- (3) **Kondoros, B. A.**; Aigner, Z. – Evaluation of fenofibrate-cyclodextrin complexes prepared by co-grinding method. III. Symposium of Young Researchers on Pharmaceutical Technology, Biotechnology and Regulatory Science, Szeged, Jan 2021
- (4) **Kondoros, B.A.**; Laczkovich, O.; Berkesi, O.; Aigner, Z. Analytical Investigation of Cyclodextrin Complexation Using the Co-Grinding Technique in the Case of Terbinafine Hydrochloride. 1st International Electronic Conference on Pharmaceutics Proceedings 2021, 78, 19. <https://doi.org/10.3390/IECP2020-08714>
- (5) **Kondoros, B. A.**; Berkesi, Ottó, Aigner, Z. – Fenofibrát tartalmú ciklodextrin-komplexek előállítása oldószer mentes technológiával és a folyamat analitikai jellemzése. Szent-Györgyi Albert Konferencia, Budapest, Apr 2021
- (6) **Kondoros, B. A.**; Aigner, Z.; Csóka, I.; Ambrus, R. – Együtt-órléssel előállított fenofibrát tartalmú ciklodextrin-komplexek vizsgálata. Magyar Kémikusok Egyesülete - Kerekasztal Konferencia, Balatonszemes, Dec 2021
- (7) **Kondoros, B.A.**; Sanzeri, G.; Bonferoni, C.; Sorrenti, M.; Csóka, I.; Ambrus, R. – Ternary Systems of Terbinafine Hydrochloride Inclusion Complexes: Preparation, Solid State Characterization, Dissolution Studies. IV. Symposium of Young Researchers on Pharmaceutical Technology, Biotechnology and Regulatory Science, Szeged, Jan 2022
- (8) **Kondoros, B.A.**; Sorrenti, M.; Csóka, I.; Ambrus, R. – Solid-state and in vitro characterization of co-ground ternary systems of Terbinafine hydrochloride. International Cyclodextrin Symposium, Giardini Naxos (Italy) Jun 2022
- (9) **Kondoros, B. A.**; Szabó-Révész, P.; Csóka, I.; Ambrus, R. – Háromkomponensű, hatóanyagtartalmú ciklodextrin-zárványkomplexek előállítása és jellemzése fizikai-kémiai és in vitro módszerekkel. Gyógyszerkémiai és Gyógyszertechnológiai Szimpózium, Herceghalom, Sept 2022
- (10) **Kondoros, B.A.**; Csóka, I.; Ambrus, R. – Investigation of the Feasibility and Efficiency of Solvent-Free Co-Grinding with Different Active Substances. V. Symposium of Young Researchers on Pharmaceutical Technology, Biotechnology and Regulatory Science, Szeged, Jan 2023
- (11) **Kondoros, B. A.**; Csóka, I.; Ambrus, R. – Különböző hatóanyagok ciklodextrines komplexeinek oldószermentes ko-órléses előállítása és vizsgálata. Magyar Kémikusok Egyesülete - Kerekasztal Konferencia, Balatonszemes, Jun 2023

ABBREVIATIONS

API	Active Pharmaceutical Ingredient
CD	Cyclodextrin
FEN	Fenofibrate
TER	Terbinafine hydrochloride
DIMEB	Heptakis-(2,6-di-O-methyl)- β -CD
HPBCD	(2-hydroxypropyl)- β -CD
SBEB CD	Sulfobutylether- β -CD
XRPD	X-ray powder diffraction
HOT-XRPD	XRPD at variable temperature
DSC	Differential scanning calorimetry
TG	Thermogravimetry
FT-IR	Fourier-transform infrared spectroscopy
SEM	Scanning electron microscopy
Ph. Eur.	European Pharmacopoeia
USP-NF	United States Pharmacopeia and the National Formulary
HPMC	Hydroxypropyl methylcellulose
PVP	Polyvinylpyrrolidone K-90
SIF	Simulated intestinal fluid
SGF	Simulated gastric fluid
CG	Co-grinding
KN	Kneading
SE	Solvent evaporation
ATR	Attenuated total reflectance
DE	Dissolution efficiency
MDT	Mean dissolution time
Caco-2	Human colorectal adenocarcinoma
PM	Physical mixture
TS	TER:SBEB CD product
TSP	TER:SBEB CD:PVP product
TSH	TER:SBEB CD:HPMC product

TABLE OF CONTENTS

1. INTRODUCTION	1
2. AIMS	2
3. LITERATURE BACKGROUND	3
3.1 Green chemical approaches for enhancing physicochemical properties	3
3.2 Cyclodextrins as molecular complexation agents	4
3.3 Using auxiliary components to prepare ternary systems with superior properties	6
3.4 Cyclodextrin complex preparation methods with or without using solvents	7
3.5 Pharmaceutical industrial application – marketed products containing cyclodextrins	9
3.6 Previous complexation approaches of the applied active ingredients	11
3.6.1. Terbinafine hydrochloride	11
3.6.2. Fenofibrate	12
4. MATERIALS AND METHODS	13
4.1 Materials.....	13
4.2 Active pharmaceutical ingredients.....	13
4.3 Excipients.....	13
4.4 Methods	15
4.4.1. Product preparation methods.....	15
4.4.2. Differential scanning calorimetry (DSC)	16
4.4.3. Thermal gravimetric analysis (TG).....	16
4.4.4. X-ray powder diffractometry (XRPD).....	17
4.4.5. Fourier-transform infrared spectroscopy (FT-IR)	17
4.4.6. Raman spectroscopy	17
4.4.7. Scanning electron microscopy (SEM)	18
4.4.8. In vitro dissolution rate studies.....	18
4.4.9. Cytotoxicity studies	19
4.4.10. Stability tests	19
5. RESULTS AND DISCUSSION	20
5.1 Complexation of Fenofibrate	20
5.1.1. Thermoanalytical evaluation of Fenofibrate products.....	20
5.1.2. Crystallographic characterization of Fenofibrate products.....	21
5.1.3. Vibrational spectroscopic evaluation of Fenofibrate products.....	22
5.1.4. In vitro studies of Fenofibrate products.....	23
5.2 Binary systems of Terbinafine HCl with cyclodextrins	24
5.2.1. Thermoanalytical characterization of binary systems of Terbinafine HCl	24

5.2.2. Crystallographic characterization of binary systems of Terbinafine HCl.....	25
5.2.3. Vibrational spectroscopic evaluation of binary systems of Terbinafine HCl.....	26
5.2.4. In vitro studies of binary systems of Terbinafine HCl.....	28
5.3 Ternary systems of Terbinafine HCl with cyclodextrins and water-soluble polymers	29
5.3.1. Thermoanalytical characterization of ternary systems of Terbinafine HCl.....	30
5.3.2. Crystallographic characterization of ternary systems of Terbinafine HCl.....	31
5.3.3. Vibrational spectroscopic evaluation of ternary systems of Terbinafine HCl	34
5.3.4. In vitro studies of ternary systems of Terbinafine HCl	36
5.4 Stability tests of prepared co-ground products	38
5.4.1. Thermoanalytical characterization during stability tests	39
5.4.2. Crystallographic characterization during stability tests	40
6. CONCLUSION.....	42
ACKNOWLEDGEMENTS.....	2

1. INTRODUCTION

The field of green chemistry strives to create chemical products in a sustainable and cost-effective manner, with the dual objective of meeting environmental and economic objectives. It is an innovative area that seeks to balance these two goals. One of the major highlights of green chemistry is minimizing or eliminating the use of solvents, as a significant amount of industrial waste generated from chemical processes is linked to solvent usage. One of the green technologies that can be easily implemented is co-grinding (CG), where mechanical force is communicated to the system using various means. Most of the publications deal with organic chemical syntheses, however, pharmaceutical intermediates from existing active pharmaceutical ingredients (APIs) have also been produced in many cases.

Cyclodextrin (CD) complexation is an intermediate preparation method, that can enhance the physicochemical properties of hydrophobic molecules, making them suitable for a diverse range of applications. Often, the aim is to increase the solubility, dissolution rate, and stability of poorly soluble APIs. Incorporating an auxiliary component during the preparation of CD complexes is an effective approach to improve complexation efficiency and enhance the therapeutic potential of various APIs. While various auxiliary components affect the mechanisms of CDs differently, the use of water-soluble polymers has been demonstrated as the most efficient method to enhance the solubilizing effect of CDs.

Traditional methods for forming molecular complexes with CDs involve using organic solvents, which can lead to additional expenses and disposal issues. Solvent-free methods are becoming increasingly important in the pharmaceutical industry, and various "green" technologies, such as microwave irradiation and mechanochemistry, are being used to create CD complexes. These methods have advantages such as reduced costs and environmental impact. Moreover, recent studies have explored solvent-free methods such as CG, which uses mechanical force to form complexes. This method can result in amorphous or partially crystalline products, depending on the grinding parameters and raw material properties. CG is considered a simple and economically desirable method for obtaining CD inclusion complexes without the need for solvents.

A comprehensive evaluation of CD complex production requires a multidisciplinary approach that incorporates a variety of analytical methods to guarantee the successful development and enduring stability of these pharmaceutical products.

2. AIMS

This Ph.D. work aims to prepare CD complexes with different model drugs by a novel, eco-friendly method, characterize this process, and compare it to conventional methods. This research was planned and carried out by the following points:

I) An extensive literature review was carried out on CD complexation especially eco-friendly, solventless preparation methods, which aimed to find less-explored alternative routes of complexation methods. Also, the literature background of different drugs was reviewed to find model drugs that were already proven to be suitable for complexation via conventional methods. Based on this review CG as a preparation method, two model drugs and several CD derivatives were selected. The preparation of amorphous products was aimed for better solubility enhancement.

II) First, the CG of Fenofibrate (FEN) was evaluated. As CD derivative Heptakis-(2,6-di-O-methyl)- β -CD (DIMEB) was selected, because pre-experiments showed that using DIMEB had the best impact on the physicochemical properties of FEN. Physicochemical and in vitro characterization was planned to characterize the product and the whole process also. A comparison of other well-known methods was also applied.

III) Secondly, a similar process and characterization were carried out on CG of Terbinafine hydrochloride (TER) with different CD derivatives. DIMEB and (2-hydroxypropyl)- β -CD (HPBCD) were selected for complexation. TER has pH-dependent solubility, so two different dissolution media were applied during in vitro tests.

IV) Based on the poor results with TER we aimed to prepare complexes with other CD derivative and apply auxiliary components also, to further enhance the positive effects of CDs. Pre-experiments showed that the combination of sulfobutylether- β -CD (SBEB CD) and water-soluble polymers have the best effect on enhancing the properties of the drug. Cytotoxicity of these products was also carried out since per os toxicity of SBEB CD is not yet fully explored.

V) Finally, we aimed to characterize the stability of complexed drugs, because amorphous products tend to recrystallize during storage. Thermoanalytical and crystallographic changes were examined in normal and accelerated stability tests for 3 months.

3. LITERATURE BACKGROUND

3.1 Green chemical approaches for enhancing physicochemical properties

One of the biggest challenges in the pharmaceutical industry is enhancing the physicochemical characteristics of drugs that have poor solubility [1]. The Biopharmaceutical Classification System (BCS) categorizes APIs into four classes based on their permeability and solubility properties [2]. APIs with poor water permeability and good permeability are classified in BCS Class II. The primary factor influencing the absorption of compounds in this category within the gastrointestinal tract is their constrained solubility and slow rate of dissolving from the formulation [3]. The inadequate solubility of these drugs can result in formulation challenges and hinder their therapeutic effectiveness, thereby increasing the possibility of bioavailability issues and dose-dependent adverse effects [4]. There are plenty of approaches to enhance physicochemical properties and avoid bioavailability issues [5], but most of them require the use of solvents, which are costly and polluting and therefore not sustainable.

Green chemistry is an innovative field that aims to produce chemical products in a sustainable, cost-competitive way to achieve environmental and economic goals at the same time [6]. Although as a cornerstone of the topic, the 12 Principles of Green Chemistry were developed as early as 1998 by Paul Anastas and John Warner [7], the subject of environmentally friendly production of materials is still a major concern today [8–10]. Among the green chemical processes are organic chemical syntheses of basic compounds and the production of intermediates, and final products [11]. It seems that chemistry, in process isolation, will not "green" the chemical processing industries, especially as represented by the pharmaceutical industry [12].

One of the most significant aspect of green chemistry is the reduction and elimination of solvents since most of the industrial waste from chemical reactions comes from solvent use [12,13]. Traditional solvents are harmful to the environment and the workers who use them. One way to reduce solvent use is to reuse them, but this is time and energy-consuming. However, the best possible way is to apply a method that achieves the same result without the use of solvents, because it eliminates the costs and problems of using solvents [14]. Furthermore, no residual solvent content could affect the quality of the products [15,16]. This is particularly important in the case of medicinal products, which has been established in a guideline to regulate this (detailed in ICH guideline Q3C (R8)) [17].

Essentially, mechanochemistry is a green method, which includes physicochemical transformations that derive from mechanical energy (compression, shear, impact, extension, etc.) [18]. The most important advantage of mechanical chemistry is the possibility of reacting substances under solvent-free conditions or using only a small amount of liquid reaction media [19]. The simplest and most common way of mechanochemical transformations is when energy is provided by grinding or milling. Both methods are suitable for mechanochemical activation. The difference is that while grinding in a mortar is a process that is difficult to reproduce, using milling machines is an automated and easily reproducible process [20].

Mechanochemical processes have several advantages over solution-based processes. Yields are often improved, and reaction rates can be faster [21]. In addition, they offer better control over the polymorphic outcome, which may not be achievable in solution-based reactions [22]. Furthermore, these reactions often proceed to completion, eliminating the need for additional purification steps [23]. Another advantage is that some mechanochemical reactions use less energy, thanks to efficient energy transfer in the reaction mixture, such as in planetary ball-milling [24]. Figure 1. summarizes the main differences based on the reviews listed above.

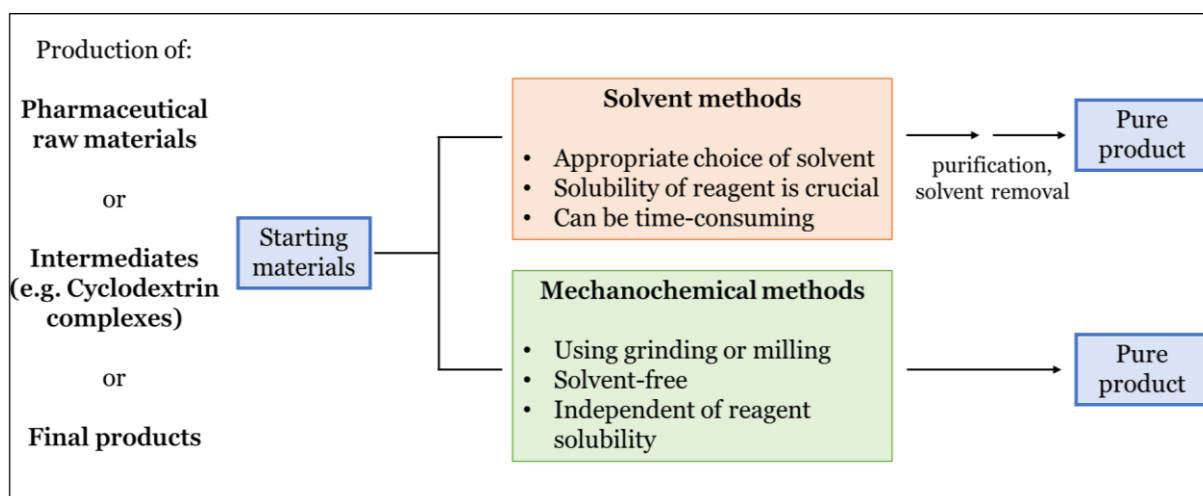


Figure 1. Main differences between solvent and solvent-free methods of product preparation in the pharmaceutical field.

3.2 Cyclodextrins as molecular complexation agents

CDs find extensive application in various industrial sectors such as cosmetics, food, and pharmaceuticals. CDs are cyclic oligosaccharides composed of α -D-glucopyranose units that are connected by α -1,4 glycoside bonds. These units take on a chair shape, resulting in a

truncated cone structure with two openings of different diameters [25]. The hydroxyl groups are located on the exterior of the molecule, with the primary and secondary ones facing the wider and narrower edges, respectively, giving the exterior a hydrophilic character. On the other hand, the CD cavity is lined with skeletal carbons and ethereal oxygens, which results in a slightly hydrophobic character. This dual nature of hydrophilic and hydrophobic characters gives CDs amphiphilic properties, making them ideal for hosting hydrophobic molecules and creating water-soluble complexes [26]. The physicochemical properties of hydrophobic molecules can be improved through complexation, making them useful for various purposes [27].

These parent CDs can be chemically modified in many ways. While natural CDs have been widely used to enhance pharmaceutical properties, chemically modified CDs (also known as CD derivatives) offer superior benefits in terms of solubility, dissolution rate, and stability [25]. Additionally, amorphous CD derivatives can be utilized to create amorphous complexes, which can improve solubility [28]. Unlike their crystalline counterparts, amorphous forms lack lattice energy and have higher configurational energies, providing better dissolution properties [29]. Therefore, amorphous properties are desirable in this point of view [30]. However, these non-crystalline materials have limited stability, and ensuring their long-term stability often poses significant challenges in drug formulation work [31].

Another main conventional application of CDs is to increase the chemical stability of complexed drugs [32]. The general perception is that CDs can enhance the chemical stability of drugs and extend the shelf-life of pharmaceutical products [33]. However, in aqueous solutions, complexation with CDs has been demonstrated to impede various types of degradation, including hydrolysis [34], oxidation [35], and photodegradation [36] of dissolved drugs. However, certain drugs, such as β -lactam antibiotics, may experience CD-catalysed degradation under specific conditions in aqueous solutions [37]. Additionally, some drugs that are stabilized by CDs in aqueous solutions may experience destabilization by the same CDs in solid dosage forms [38]. As a result, it is necessary to assess and confirm the effects of CDs on drug stability in the final drug formulation and under recommended storage conditions [39].

In addition to their conventional function, CDs can also be included as APIs in medicinal products. Numerous research is also being carried out on this aspect. Some of these innovative preparations are on the market for the unblocking of neuromuscular block under anaesthesia (Sugammadex) and for the treatment of Niemann Pick Type C disease (HPBCD) [40].

Evaluating CD complex production requires a multidisciplinary approach, utilizing a range of analytical methods to ensure the successful creation and long-term stability of these important pharmaceutical products [41,42]. The investigation of potential complexes requires X-ray powder diffraction (XRPD) studies as well as thermal analysis using differential scanning calorimetry (DSC) and thermogravimetry (TG) [43–46]. Additionally, spectroscopic techniques such as Fourier-transform infrared (FT-IR) and Raman spectroscopy can provide valuable supporting information. Scanning electron microscopy (SEM) measurements have also been demonstrated to be beneficial in explaining and improving the understanding of solid phase changes [47–50].

3.3 Using auxiliary components to prepare ternary systems with superior properties

Binary systems consisting of the APIs and CDs are commonly used in pharmaceutical applications, while supramolecular systems known as ternary CD complexes are composed of three distinct materials [51]. Adding an auxiliary component in the preparation of CD complexes is an adequate strategy to increase the complexation efficiency and promote the therapeutic utility of different APIs [52]. These multicomponent systems contain amino acids, organic acids or bases, or water-soluble polymers as a second excipient, further improving the beneficial properties of CDs [53]. As a result of physicochemical, solubility, and transport properties with these new formulations, higher drug administration and reduction of the amount of API and/or CD can be achieved [54]. Thereby auxiliary components are tools to optimize the cost, toxicity, and formulation volume in the final product.

Different types of auxiliary components influence the effects of CDs in different mechanisms [51,53,55]. However, using water-soluble polymers has proven to be the most effective way to increase the solubilising effect of CDs [56]. Polymers can act on their own to increase solubility and are widely used in the pharmaceutical industry for this reason and many more [57]. However, they can also interact with the outer surface of CDs and thus with CD complexes. The resulting API-CD-polymer co-complexes have a stability constant that exceeds that of binary products, thus increasing their solubilisation efficiency [58]. Several studies have shown that the obtained ternary systems increase the in vitro solubility properties compared to both polymer-containing and CD binary products, thus a synergistic effect can be presumed [59]. PVP and HPMC have been widely studied for this purpose as easily available polymers in ternary systems.

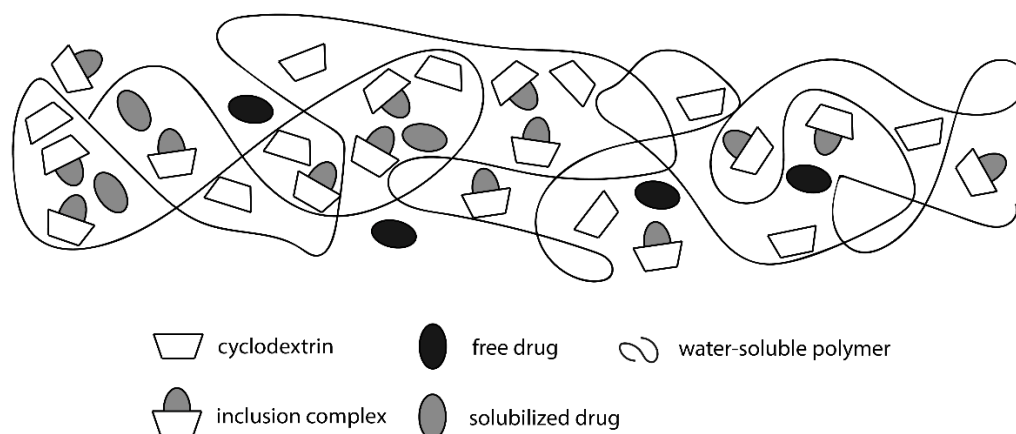


Figure 2. Schematic representation of water-soluble polymer containing CD ternary systems

3.4 Cyclodextrin complex preparation methods with or without using solvents

Typically, conventional methods for preparing molecular complexes with CDs involve using a specific quantity of organic solvent [60]. This solvent mixture is used to dissolve all or a portion of the components so that a secondary bond can form between the molecules, ensuring sufficient stability of the inclusion complex [61].

Generally, all the materials are dissolved using a defined amount of organic solvent in conventional methods of forming a molecular complex with CDs. To promote the formation of the inclusion complex, the solution can be cooled slowly or added drop by drop to a solvent that maintains low solubility of the complex. Alternatively, the pH of the solution can be adjusted to facilitate the precipitation of the complex. Afterward, the precipitate is washed with an appropriate solvent and dried [60].

However, in the case of kneading (KN), only a small amount of solvent mixture is used. The KN process is utilized to improve manufacturability and blend uniformity. Depending on the desired scale, KN can be accomplished using a mortar and pestle, as well as planetary or high-shear mixers. The procedure involves mixing CD with enough water to create a slurry or uniform paste, then adding the API as a solid or a pre-dissolved aqueous solution to the slurry, and ultimately blending the components [1,62].

The process of purchasing, storing, disposing of organic solvents, and controlling residual solvent content in the final product can be costly in terms of time, materials, and energy. Additionally, the use of solvents can result in unwanted reagent consumption via hydrolysis

[63]. As a result, many industries, including pharmaceuticals, favour organic solvent-free preparation methods due to these drawbacks [13]. Solid-state processes that do not require solvents, or only use minimal amounts of solvent (catalytic amounts), have gained significant attention lately. Green technologies such as microwave irradiation, sonochemistry, photochemistry, and mechanochemistry are becoming increasingly important for producing CD complexes [64].

In recent research, alternative techniques that eliminate the need for solvents, such as CG, have been investigated. CG involves employing mechanical energy to produce the complexes [65]. By avoiding solution-based methods, this approach offers added benefits and avoid challenges, including problems with solvent complexation, and solvolysis. In addition to reducing the use of solvents, CG is also preferred when the product or a certain polymorph of the product cannot be produced by classical methods. Moreover, in many cases, this method can provide a faster route to higher yields [66,67].

The mortar and pestle are the primary tools used for grinding (Figure 3.a). Although the energy input is not easily measurable, grinding proved to be an effective technique for preparing CD complexes in the solid state. Various examples show amorphization and complexation of different APIs using mortar and pestle [47,68]. Vibrational mills are capable of operating batch-wise and are appropriate for preparing laboratory products on a scale of grams (Figure 3.b). The effect achieved by vibrational mills is typically attributed to several factors, including the frequency of the vibrating motion, the milling time, the material of the milling balls, their density, and the ratio of milling media to charge [69]. Several articles deal with the CD complexation of APIs by vibratory milling and the effects of the mentioned variable parameters [46,70]. Another well-known instrument is the planetary mill, where the variation in velocities between the grinding jars and balls results in an interplay of frictional and impact forces, generating significant dynamic energies (Figure 3.c). In contrast to the vibrational milling, the parameter variable is the rotation speed instead of the vibration frequency and in addition to laboratory-scale devices, pilot-plant scale production is also possible. Scientific work on CD complexation is also being carried out extensively with planetary mills [71,72].

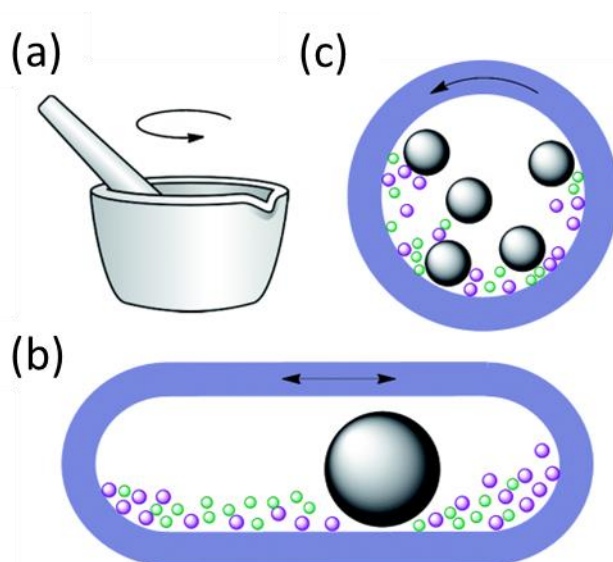


Figure 3. Illustrations of the three primary tools of CG: (a) grinding with mortar and pestle; (b) high-speed vibration milling in a mixer mill; (c) planetary ball milling [73].

3.5 Pharmaceutical industrial application – marketed products containing cyclodextrins

There are basically 3 main directions in pharmaceutical research: original, generic and - to a lesser extent – “Supergenerics”. While generics have the same bioavailability as the originator product, “Supergenerics” are concerned with the development and commercialisation of APIs with improved properties [74]. By 2030, the sales of these advanced drug formulations in the pharmaceutical industry could potentially reach up to US\$ 365 billion [75].

CD-containing pharmaceutical products are widely used due to their ability to improve the solubility and bioavailability of hydrophobic drugs as an attempt to formulate “Supergenerics”. Publications related to CDs and their various applications have been steadily increasing since 1975, as shown in Figure 4. The graph shows 5-year intervals, but the last column shows only the 3 years from 2020 to the writing of this thesis. There was a slight decrease in the time interval between 2015-2020. However, in just 3 years since then, there has been an increase again. This surge in publications can be attributed in part to the more cost-effective and efficient production of CDs in the industry.

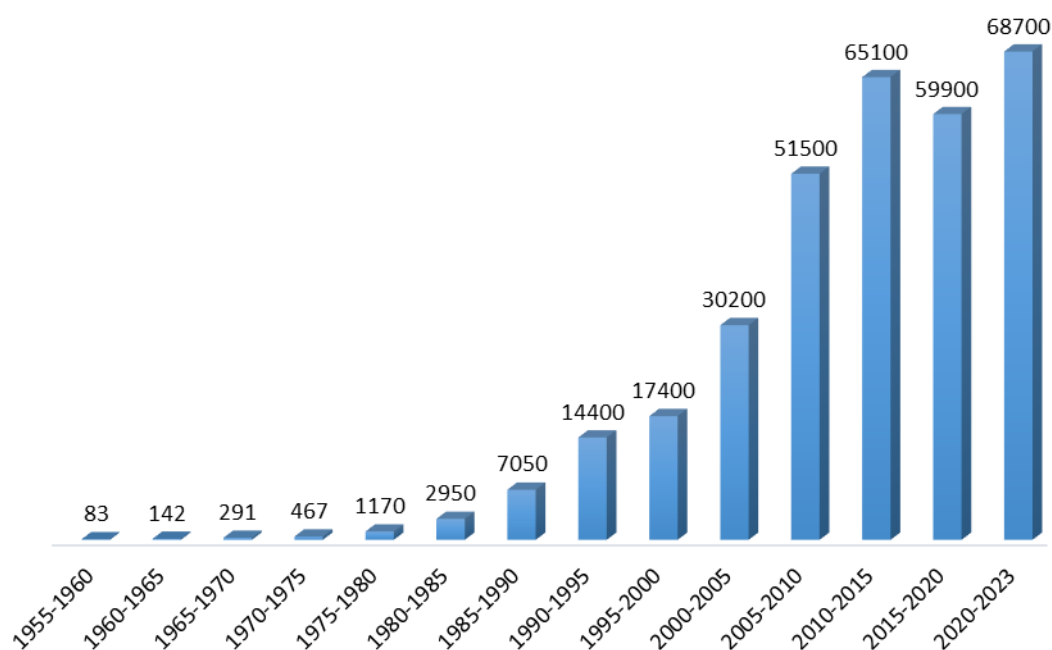


Figure 4. The growing trend of CD publications between 1955 and 2020 (using the keyword "cyclodextrin" on Google Scholar)

The first patent recorded was in the early 1980s, when a slow increase in CD patents was noted throughout the decade. Nevertheless, the pharmaceutical sector witnessed a remarkable surge in the adoption of CDs in the early 2000s [76]. There are four main categories in which current patents for CDs can be classified. The first category consists of patents for methods of producing CDs. The second category includes patents for pharmaceutical applications of certain CD derivatives. For instance, Johnson & Johnson holds a patent for the pharmaceutical use of HPBCD in the US, while CyDex holds a patent for SBEB CD. The third category comprises patents for methods aimed at enhancing the performance of CDs, such as certain ternary system formulation techniques involving adding hydroxy acids or water-soluble polymers to improve their solubilizing effects. Finally, the fourth category encompasses patents for specific drug/CD combinations. This is the largest category, accounting for more than a third of all CD-related patents [77].

Together with the publications and patents, the range of CD-containing drugs marketed has also increased greatly. The first pharmaceutical product containing CD, commercialized in Japan in 1976, was Prostarmon E™ (prostaglandin E2 with βCD) [78]. Table 1. provides a summary of some of the medicinal products containing CD that are already on the market since

then. In addition to these, there are more than 120 similar formulations on the market worldwide [79], but the scope of this paper does not allow a complete list to be presented.

Table 1. A brief review of marketed products containing CD as excipient based on the work of Puskás et al. [79].

Drug	CD	Trade name	Dosage form	Company
Cetirizine	β -CD	Zyrtec, WalZyr, Revicet	chewing tablet, orally dissolving tablet, dry syrup	Losan Pharma, UCB Pharma, Sandoz, etc. Karalex
Fenofibrate	β -CD	Fenofibrate, Fenacor, Fibrate, Lipicard, etc.	tablet, capsule, injection	Pharma, Avinash Health, etc.
Voriconazole	SBEB CD	Vfend, Voriconazole (veterinary) Jcovden (previously	i.v. solution	Pfizer, Sandoz
Ad26.COVS.2.S	HPBCD	COVID-19 Vaccine (Janssen)	vaccine	J&J
Estradiol	RAMEB	Aerodiol	nasal spray	Servier
Cisapride	HPBCD	Prepulsid	suppository	Janssen

The market is dominated by β -CD and its derivatives, including hydroxypropylated and sulfobutylated variants such as HPBCD and SBEB CD. While HPBCD was the first semi-synthetic derivative of CD to be used in final dosage forms, SBEB CD has become increasingly popular due to its powerful solubilizing and stabilizing properties. CDs can be used in all routes of administration, from per os tablets to eye drops and parenteral vaccines [60]. However, there is no evidence that SBEB CD-containing per os medicines are on the market.

3.6 Previous complexation approaches of the applied active ingredients

3.6.1. Terbinafine hydrochloride

Terbinafine is an antifungal medication that works by inhibiting the squalene-epoxidase enzyme, which is essential for the synthesis of ergosterol, an important component of fungal cell membranes [80]. This drug can be administered both topically and systemically and one of the advantages of terbinafine is its ability to accumulate in the hair and nails during systemic

administration, making it particularly effective in treating fungal infections of the nails [81,82]. Common side effects of terbinafine therapy include gastrointestinal complaints, taste loss, and cutaneous adverse effects such as rash or itching [83–85]. In addition to these common side effects, elevations in liver enzymes and bilirubin have also been observed in some patients taking terbinafine, and acute hepatitis has been reported in rare cases [86].

Because of its poor water solubility, its hydrochloride salt is used in pharmaceutical preparations on the market. However, even the more soluble hydrochloride salt is BCS Class II, and its pH-dependent solubility is particularly problematic. Several studies have shown that CD complexation can increase the stability and solubility of terbinafine, making it a promising approach for the formulation of this drug [87,88]. However, the solvent-free conditions to produce the API-CD complex have not yet been developed.

3.6.2. Fenofibrate

Fenofibrate (FEN) is a widely used antidyslipidaemic drug for lowering blood cholesterol and triglycerides levels [89]. The most common side effects of FEN include gastrointestinal symptoms such as nausea, diarrhea, and abdominal pain. Other potential side effects include muscle pain or weakness, liver problems, and an increased risk of developing gallstones [90,91]. It was marketed for the first time in 1975 and is currently being marketed in approximately 85 countries worldwide [92].

There are four known polymorphs of FEN that exhibit distinct physical characteristics, and among these, three have been observed to possess limited thermal stability [93]. This API belongs to BCS Class II, because of its low water solubility, causing low bioavailability [94]. This property can be effectively improved by CDs so that the dosage applied can be reduced, thus reducing side effects. For this reason, several articles deal with the solubility and bioavailability enhancement of FEN [95]. Previous works have also demonstrated the feasibility of CD complexation. However, these scientific publications have always used solvent-based methods [96,97]. Aigner et al. have previously studied and shown that DIMEB has the most solubilising effect on FEN among the various CD derivatives [98].

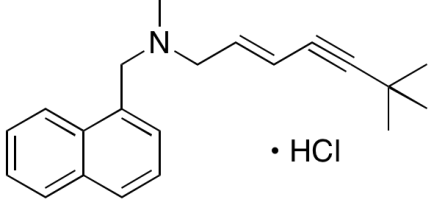
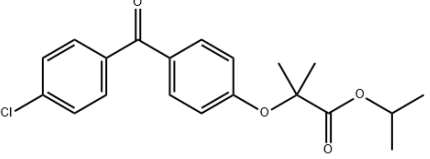
4. MATERIALS AND METHODS

4.1 Materials

4.2 Active pharmaceutical ingredients

Terbinafine hydrochloride (TER) and Fenofibrate (FEN) was kindly donated by Gedeon Richter Plc. (Budapest, Hungary).

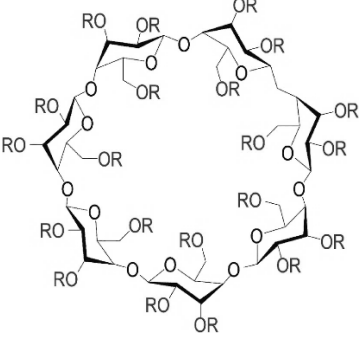
Table 2. The physicochemical and pharmaceutical properties of the drugs were used.

Name of API	Terbinafine HCl (TER)	Fenofibrate (FEN)
Chemical structure		
Chemical name	(E)-N,6,6-trimethyl-N-(naphthalene-1-ylmethyl) hept-2-en-4-yn-1-amine hydrochloride	isopropyl-2-[4-(4-chlorobenzoyl)phenoxy]-2-methylpropanoate
Formula	C ₂₁ H ₂₅ N.HCl	C ₂₀ H ₂₁ ClO ₄
M _w	327.9	360.8
Melting point	204-208 °C	80-81 °C
logP	5.53	5.30
Solubility in water		<0.1 mg/mL
BCS class ^a		BCS class II.
Pharmacology	Antifungal medication used to treat pityriasis versicolor, fungal nail infections	Used to treat abnormal blood lipid levels.

4.3 Excipients

Different type of CD-derivatives was used in the studies discussed below. Heptakis-(2,6-di-O-methyl)-β-CD (DIMEB) was kindly donated by Cyclolab R&D Laboratory Ltd. (Budapest, Hungary). Sulfbutylether-β-CD (SBEB CD) was provided by Sanofi-Aventis Ltd. (Paris, France). (2-hydroxypropyl)-β-CD (HPBCD) was purchased from Wacker Chemie AG (Munich, Germany).

Table 3. The physicochemical and pharmaceutical properties of the CDs were used.

Name of CD	Heptakis-(2,6-di-O-methyl)- β -CD (DIMEB)	(2-hydroxypropyl)- β -CD (HPBCD)	Sulfobutylether- β -CD (SBEB CD)
Chemical structure			
Formula	$R=H$ or CH_3 $C_{42}H_{70-n}O_{35} \cdot (CH_3)_n$	$R=H$ or C_3H_7O $C_{42}H_{70-n}O_{35} \cdot (C_3H_7O)_n$	$R=H$ or $C_4H_8O_3SNa$ $C_{42}H_{70-n}O_{35} \cdot (C_4H_8O_3SNa)_n$
Type	nonionic	nonionic	anionic
M_w	$1135.0 + n \cdot (14.0)$	$1135.0 + n \cdot (58.1)$	$1135.0 + n \cdot (158.2)$
Degree of substitution	14.0	6.3	2.0
LogP	unavailable	-11 [99]	<-10 [99]
F_{oral}^a	unavailable	≤ 0.03 [25]	0.02 [25]
Solubility in water	highly soluble	> 600 mg/mL [25]	> 500 mg/mL [25]
Max. dosage in marketed drug products	unavailable	8000 mg/day [100]	3600 mg/day [101]
Pharmacopoeia monographs ^b	none	Ph.Eur., USP-NF	Ph.Eur., USP-NF

^a Fraction of CD excreted unchanged with the urine after parenteral administration to humans.

^b The European Pharmacopoeia (Ph.Eur.), the United States Pharmacopoeia and the National Formulary (USP-NF)

Hydroxypropyl methylcellulose (HPMC) was kindly supplied by Colorcon (Dartford, UK). Polyvinylpyrrolidone K-90 (PVP) molecular weight: 1300000 was received as a gift from Gedeon Richter Plc. (Budapest, Hungary).

For buffer preparation simulated intestinal fluid (SIF) and simulated gastric fluid (SGF) without enzymes were prepared based on Chapter 5.17.1 of the Ph.Eur. (10th edition). For the preparation of SIF (pH 6.8) 77.0 mL of 0.2 M NaOH, 250.0 mL of an aqueous solution containing 6.8 g of KH_2PO_4 , and 500 mL of purified water were mixed, pH was adjusted to pH 6.8 and diluted to 1000 mL with purified water. SGF (pH 1.2) was prepared as follows: 1 g of NaCl was dissolved in purified water and 80 mL of 1 M HCl was added; finally, the solution was diluted to 500 mL with purified water. To prepare 1 L of phosphate buffer solution (PBS) 1.44 g of disodium phosphate dihydrate ($\text{Na}_2\text{HPO}_4 \times 2 \text{H}_2\text{O}$), 0.12g potassium dihydrogen phosphate (KH_2PO_4), 8.00 g sodium chloride (NaCl), and 0.20 g potassium chloride (KCl) were dissolved and diluted to 1000 mL with distilled water. All materials used for these solutions were purchased from Sigma-Aldrich (Budapest, Hungary).

4.4 Methods

4.4.1. Product preparation methods

The first critical issue regarding the design of the product preparation reported in this thesis was the determination of the API to CD molecular ratio of the complexes for substances to be investigated. Based on the literature and our own preliminary experiments, complexes with a molecular ratio of 1:1 are formed with both APIs and the CD used. To accurately calculate the substances to be measured, water content was determined for each CD derivative. The moisture contents of the CDs were measured at 105 °C using a Mettler-Toledo HR73 (Mettler-Toledo Ltd., Budapest, Hungary) halogen moisture analyzer.

Each time, after determining the exact materials to be measured, a physical mixture (PM) was prepared, and samples of the PM were taken for later analysis. Different solvent and solvent-free complexation methods were then performed based on these PMs.

To achieve a lightweight and uniform product, an agate mortar was utilized for CG. The time of CG process was determined through preliminary tests. At intervals of 5 minutes, suitable sample quantities were collected for physicochemical analysis. During CG, samples were taken every 5 minutes and XRPD tests were performed simultaneously. Grinding was continued until an amorphous product was obtained. These grinding times varied depending on API and CD,

but the final products always had amorphous characteristics. Grinding amorphous materials below their glass transition temperature can produce an amorphous phase while grinding at higher temperatures is more likely to lead to metastable polymorphic forms [22]. Therefore, the CG preparation method was carried out at room temperature and pauses were included at fixed intervals to avoid heating due to friction. The grinding times mentioned in the thesis do not include these pauses, only the time spent on effective grinding.

For the preparation tool of the inclusion complex using the KN method mortar was used. However, this time a minimal amount of 50% (v/v) ethanol-water mixture was employed. Once the liquid phase was added, the suspension system was continuously stirred until a significant portion of the liquid had evaporated. The resulting product was subsequently dried in a vacuum drier at room temperature for 24 hours and then finely powdered with care. The solvent evaporation (SE) products were prepared by completely dissolving the PM in 50%(v/v) ethanol-water mixture and evaporating the solvent in a vacuum drier at room temperature for 24 hours.

The production of ternary systems was similar. The only difference was in the calculation of the PM composition. Here, the predetermined amount to be prepared had a given polymer (PVP or HPMC) content of either 5 or 15 w/w%. The remaining 95 or 85 w/w% also contained API:CD in a 1:1 molar ratio, also taking into account the water content.

4.4.2. Differential scanning calorimetry (DSC)

The DSC analysis was performed with a Mettler-Toledo DSC 821e instrument (Greifensee, Switzerland), the heating rate was 5 °C min⁻¹, in the temperature interval of 25–300 °C, argon was used as a carrier gas (10 L h⁻¹). All samples and raw materials were characterized with these parameters, the investigated quantity was in the range of 2–5 mg, and examinations were performed in sealed Al pans of 40 µL with three leaks.

4.4.3. Thermal gravimetric analysis (TG)

Thermogravimetric analysis (TG) was performed with Mettler–Toledo TGA/DSC1 (Mettler–Toledo GmbH, Switzerland) instrument. The weight of the samples ranged from 5.0 to 5.5 mg. Samples were heated from 25 to 300 °C with a heating rate of 10 °C min⁻¹.

The evaluation of all measurements was performed with STARe VER 9.30 software for both DSC and TG experiments.

4.4.4. X-ray powder diffractometry (XRPD)

For XRPD measurements a Bruker D8 Advance diffractometer was used. The measurements were performed with Cu-K α I radiation at a wavelength of 1.5406 Å, X-ray tube voltage was 40 kV and 40 mA. Diffractograms were recorded in the angular range of 3-40° (2 θ) with a pitch of 0.007° and a time constant of 0.1 s. The obtained data were evaluated with the Bruker DiffracPlus Eva software.

The alteration in crystal structure resulting from temperature fluctuations was observed using XRPD (HOT-XRPD) fitted with an MRI Basic hot-humidity chamber (MRI Physikalische Geräte GmbH, Karlsruhe, Germany) that was regulated by an Ansyco Sycos H-Hot system (Analytische Systeme und Komponenten GmbH, Karlsruhe, Germany). HOT-XRPD measurements were conducted within a temperature range of 30–240 °C, with intervals of 5 °C. The humidity remained constant at the ambient level throughout the experiments, which were carried out under typical room conditions.

4.4.5. Fourier-transform infrared spectroscopy (FT-IR)

Spectra were recorded on different types of spectrophotometers equipped with attenuated total reflectance (ATR) devices. Measurements were performed between 4000 and 400 cm⁻¹, at an optical resolution of 4 cm⁻¹, and 256 scans were averaged to increase the signal-to-noise ratio.

Spectral manipulations were performed by using Thermo Scientific GRAMS/AI Suite software (version 9.0) and Spectragryph - optical spectroscopy software [102]. Subtracting atmospheric water vapor superimposed on the sample spectrum was performed using a measured water vapor spectrum.

4.4.6. Raman spectroscopy

Raman spectra were recorded with a Thermo Fisher DXR Dispersive Raman spectrometer (Waltham, USA) equipped with a CCD camera and a diode laser ($\lambda = 780$ nm). The following parameters were used during the measurements: the applied laser power was 12 and 24 mW at 25 μ m slit aperture size; spectra were collected with an exposure time of 6 sec. The data were collected in the spectral range of 3300–200 cm⁻¹ using automated fluorescence corrections. OMNIC for Dispersive Raman 8 software package (Thermo Fisher Scientific, Waltham, USA) was used for data collection, averaging a total of 20 scans. For the removal of cosmic rays, a convolution filter was applied to the original spectrum using a Gaussian kernel.

In addition to recording individual spectra, the Raman mapping method was also applied to obtain images of the distribution of the ingredient in the samples. Spectra were collected using a five times six grid from the 750 times 250 μm size area of the samples, defined by the optical microscope.

4.4.7. Scanning electron microscopy (SEM)

The morphological aspects of the products were studied by scanning electron microscopy (SEM; Hitachi S4700, Hitachi Scientific Ltd., Tokyo, Japan) at 10 kV on samples previously coated with a thin film (about 10 nm) of gold-palladium from a coater sputter (Bio-Rad SC 502, VG Microtech, Uckfield, UK). The results were obtained using ImageJ 1.44p software (Bethesda, MD, USA). Statistical analysis was performed to determine the existence of a significant difference between the measured data. For all characterized products, unidirectional variance analysis (ANOVA) was performed with the post hoc Tukey HSD test. In the same way, the particle diameters of the samples produced by different preparation methods were examined. Experimental results with p-values <0.05 and <0.01 were assumed to be statistically significant.

4.4.8. In vitro dissolution rate studies

Dissolution rate studies of pure drugs and prepared solid inclusion complexes, and marketed products were carried out. According to European Pharmacopeia dissolution studies were performed in a dissolution apparatus with a paddle method at 37 $^{\circ}\text{C}$ by applying 100 rpm but in a reduced volume of medium (50 mL). Aliquots were withdrawn and replaced with fresh dissolution medium at given times (5, 10, 20, 30, 60, 90, and 120 min) and immediately filtered (syringe membrane filter with a pore size of 0.22 μm). After proper dilution with the dissolution medium, the concentration of the dissolved drug was determined using a Unicam UV/VIS spectrometer (Thermo Fisher Scientific, Waltham, MA, USA).

Cumulative dilution caused by the medium replaced during sampling has been considered. To quantify the dissolution curves, two metrics were used, dissolution efficiency (DE) and mean dissolution time (MDT), calculated according to the following equations. DE represents the area under the dissolution curve up to a specified time and it is expressed as a percentage of the rectangle area and can be calculated using the equation:

$$\text{DE} = \frac{\int_0^t y \, dt}{Y_{100}} 100\% \quad (2)$$

MDT is used to characterize the drug release rate of the APIs and the products, using the following equation:

$$MDT = \frac{\sum_{i=1}^n t_{mid} \Delta M}{\sum_{i=1}^n \Delta M} \quad (3)$$

4.4.9. Cytotoxicity studies

To characterize cell viability, the mitochondrial activity was measured using an MTT (3-(4,5-dimethylthiazol-2-yl)-2,5-diphenyltetrazolium bromide) assay in 96-well cell culture microplates using Caco-2 (human colorectal adenocarcinoma) cells. Caco-2 cells were seeded at a density of 4×10^4 cells/well. Two-fold serial dilution of compounds has been prepared with a maximum TER concentration of 1 mg/mL to 0,001953 mg/mL. Afterward, samples were incubated at 37 °C for 24 h. Later, 20 μ L of MTT was added to each well. After an additional incubation at 37 °C for 4 h, 100 μ L of 10% sodium dodecyl sulfate was added and after 12 h incubation, the optical density (OD) was measured. Cytotoxicity was then determined by measuring the OD at 550 nm (ref. 630 nm) with EZ READ 400 ELISA reader (Biochrom, Cambridge, UK). The viability of untreated cells corresponded to 100% and the viability of products was compared to this control. The assay was replicated four times for each concentration.

4.4.10. Stability tests

Amorphous materials are thermodynamically unstable forms due to their high Gibbs energy, and this instability can lead to recrystallization [103]. The stability of the products was investigated under different conditions because of the expected instability of the amorphous materials. They were investigated at room temperature and for accelerated stability tests: 40 °C and relative humidity of 75% in a KKS TOP+ climate chamber (POL-EKO-APARATURA, Wodzisław Śląski, Poland) for 3 months. Stored products were evaluated by DSC and XRPD methods to reveal changes in the crystal structure, thermal behaviour, and intermolecular interactions.

5. RESULTS AND DISCUSSION

5.1 Complexation of Fenofibrate

The complexation of FEN was experimented with DIMEB and studies were carried out to investigate the complexation effect and the change of the investigated properties as a function of time.

5.1.1. Thermoanalytical evaluation of Fenofibrate products

FEN thermogram contains a sharp peak around 80.5 °C indicating the melting point of the API. The test does not indicate any decomposition of the melted substance at higher temperatures. On the DIMEB thermogram, a broad and flat drop in temperature range between 25 and 70 °C is observed, which is due to the presence of moisture in the material. No further changes in temperature can be detected above 70 °C (Figure 5.a). As the endothermic peaks of DIMEB and FEN do not overlap, the thermally-induced changes resulting from CG can be investigated.

The thermogram of the PM (0 min grinding) of FEN and DIMEB shows the endothermic peak of the drug's melting point. The presence of the complexing component widens the peak, and the area beneath the curve decreases proportionally to the weight ratio of the two-component product. As the grinding time progresses, the area under the curve corresponding to the drug's melting point diminishes, indicating a gradual reduction in the amount of crystalline drug. After 60 minutes of CG, it becomes challenging to detect the presence of crystalline API (Figure 5.b).

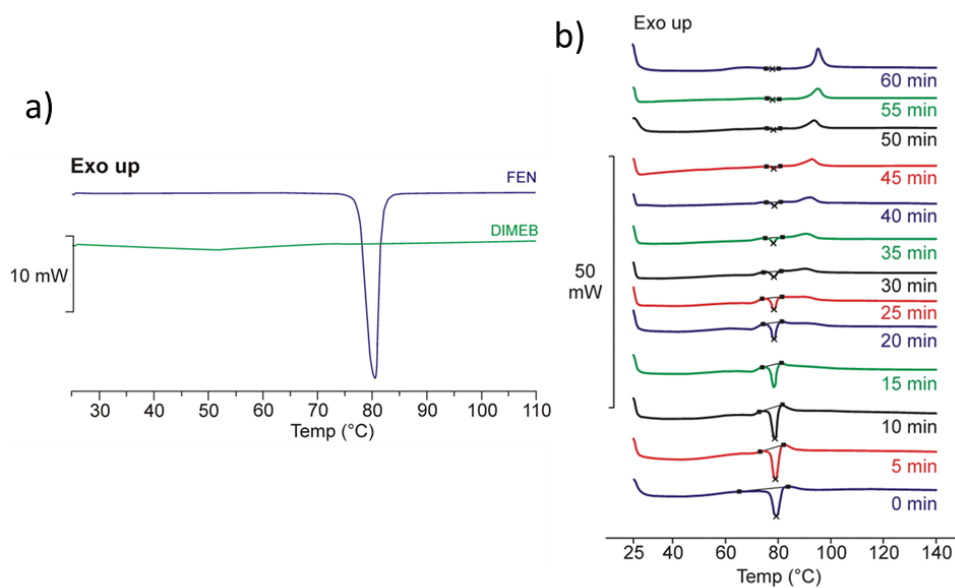


Figure 5. DSC diffractograms of starting materials (a) and series of samples from 0 to 60 minutes grinding time (b).

5.1.2. Crystallographic characterization of Fenofibrate products

XRPD diffractograms were obtained for both the PM and the CG products. FEN exhibited well-defined characteristic peaks, indicating its crystalline nature and belonging to polymorph I according to the Cambridge Structural Database. On the other hand, DIMEB displayed a completely amorphous structure with no sharp peaks. The PM of FEN and DIMEB exhibits distinct peaks characteristic of the drug, which overlay the amorphous diffractogram of CD. The intensity of these peaks reflects the FEN content in the two-component product. Through 60 minutes of CG, the intensity of these peaks gradually decreasing, leading to the amorphous nature of the product (Figure 6.). This finding aligns with the continuous decrease and eventual absence of the endothermic peak at the melting point of FEN observed in the DSC studies. The DSC and XRPD tests don't provide conclusive information regarding whether amorphization or molecular complexation during CG is responsible for the decrease in the area under the endothermic peak. To confirm this, additional studies such as FT-IR should be used. The KN method did not succeed in obtaining a completely amorphous product, but a partially crystalline product. (data not shown).

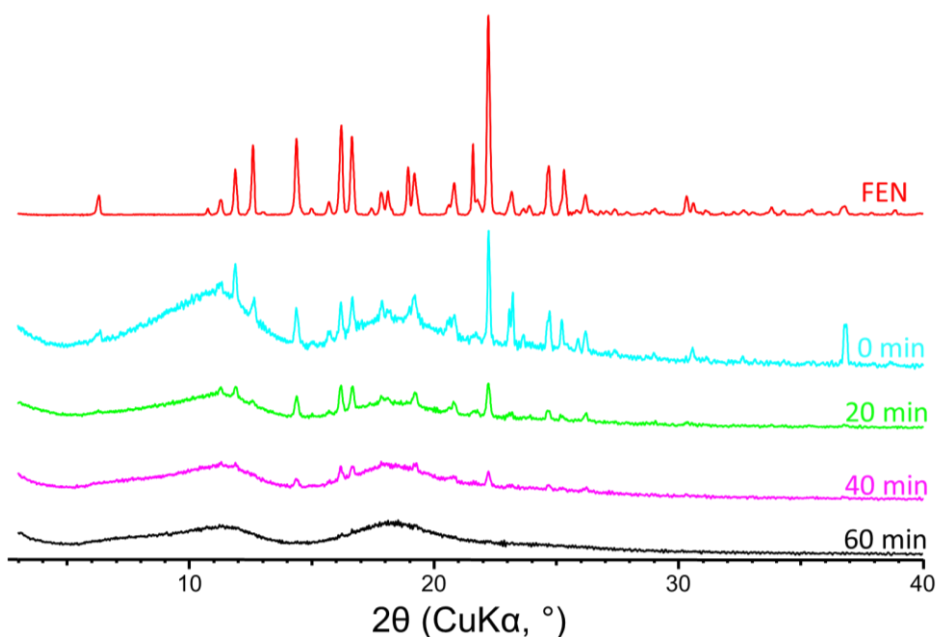


Figure 6. XRPD diffractograms of FEN (polymer I.), PM (0 min), and CG samples are shown every 20 minutes until complete amorphization at 60 minutes.

5.1.3. Vibrational spectroscopic evaluation of Fenofibrate products

The grinding process led to complex changes in the FTIR spectra of the samples, making it difficult to interpret the results using simple methods such as spectral subtraction or more advanced techniques like Fourier deconvolution or peak fitting. However, by constructing a dynamic surface using normalized spectra (Figure 7.), it became apparent that the grinding process could be examined in three distinct 20-minute intervals.

The changes in intensity indicated that the behaviour of the peaks could be grouped into three categories based on the grinding time. Some peaks exhibited increasing intensities, while others showed decreasing intensities. Additionally, some peaks reached their maximum intensity around the middle of the grinding time. During the grinding process, it appeared that the first and last 20 minutes were primarily influenced by a single dominant process. In contrast, the middle 20 minutes indicated a combination of multiple processes occurring simultaneously.

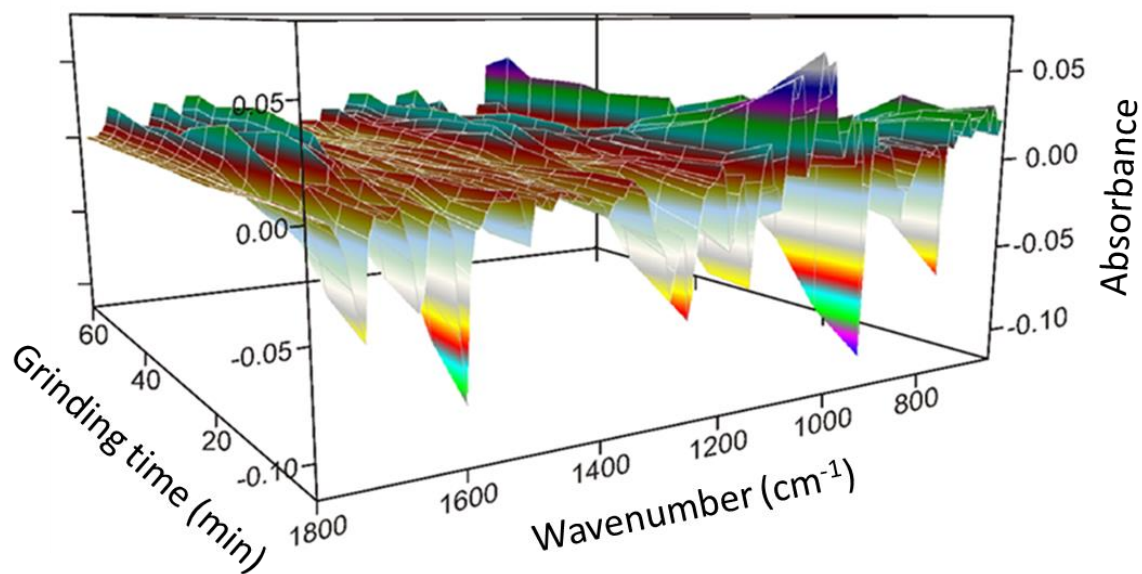


Figure 7. The dynamic surface (the different colours of the surface produced by the 3D representation belong to the values of the Y-axis), was constructed from the truncated and normalized spectra between 1800 and 630 cm^{-1} and recorded between 0 and 60 min of the grinding time interval.

5.1.4. In vitro studies of Fenofibrate products

Dissolution studies were carried out using modified pharmacopeia methods in SIF. Figure 8 illustrates the dissolution curves of the pure drug and its equimolar products, while Table 1 presents the corresponding calculated DE values. FEN on its own demonstrated minimal solubility in this aqueous solution. All binary systems exhibited improved dissolution properties compared to the pure drug. The PM showed enhanced solubility compared to the API alone, attributed to the presence of a small concentration of dissolved CD in the medium. Nevertheless, this improvement was limited. In contrast, the KN and CG products achieved a much greater increase in solubility. The CG product exhibited a faster dissolution rate and slightly better solubility compared to the kneaded product.

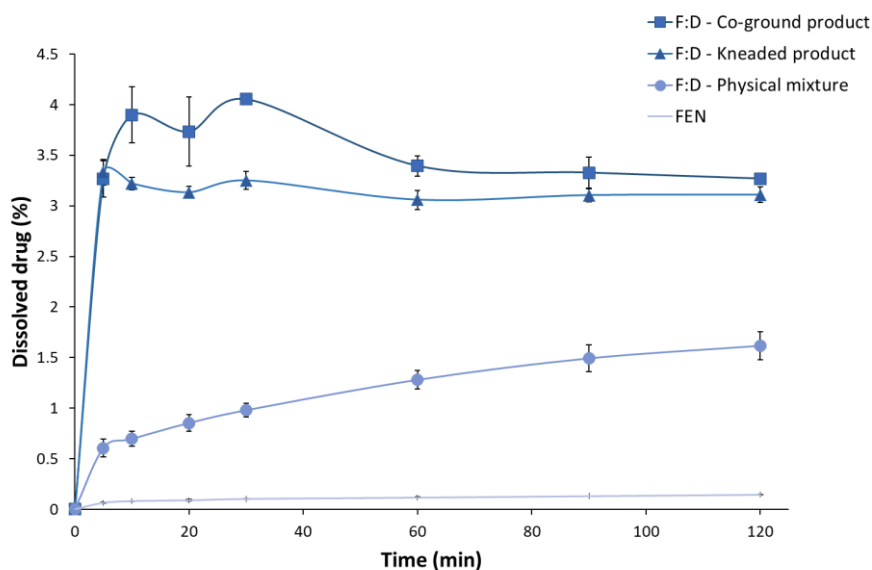


Figure 8. Dissolution curves of FEN, PM, KN, and CG products in SIF.

Table 4. Calculated DE at 60- and 120-minutes during dissolution studies.

	DE 60 min (%)	DE 120 min (%)
FEN	0.09±0.01	0.11±0.01
F:D – physical mixture	0.94±0.09	1.20±0.12
F:D – kneaded	3.05±0.10	3.07±0.09
F:D – co-ground	3.59±0.10	3.46±0.11

5.2 Binary systems of Terbinafine HCl with cyclodextrins

This part of the thesis aimed to prepare CG products and follow through the preparation process of the CG method with analytical tools in the case of TER and two amorphous CD derivatives: HPBCD and DIMEB.

5.2.1. Thermoanalytical characterization of binary systems of Terbinafine HCl

Figure 9.a displays the DSC thermograms of TER, DIMEB, and all samples obtained during the CG process with these materials. Figure 9.b illustrates the same scheme for products containing HPBCD. At lower temperatures, both CDs exhibit a broad endothermic signal (25–85 °C), indicating the presence of water in the CD derivative. DIMEB also exhibits an exothermic peak at 187 °C, indicating a crystallographic phase transition. The DSC data reveals a distinct peak corresponding to the melting point of TER near 209 °C, as well as a complex phenomenon at higher temperatures, suggesting TER degradation. These peaks are separate, allowing the detection of thermoanalytical changes related to the process. Products containing DIMEB show a complex thermoanalytical signal below the melting point of the API. This peak

broadens with longer grinding time and can be detected in the final product at 150–190 °C. In the case of HPBCD, this phenomenon is absent, but a broad complex endothermic peak appears between 220 and 260 °C, likely associated with the degradation of the API.

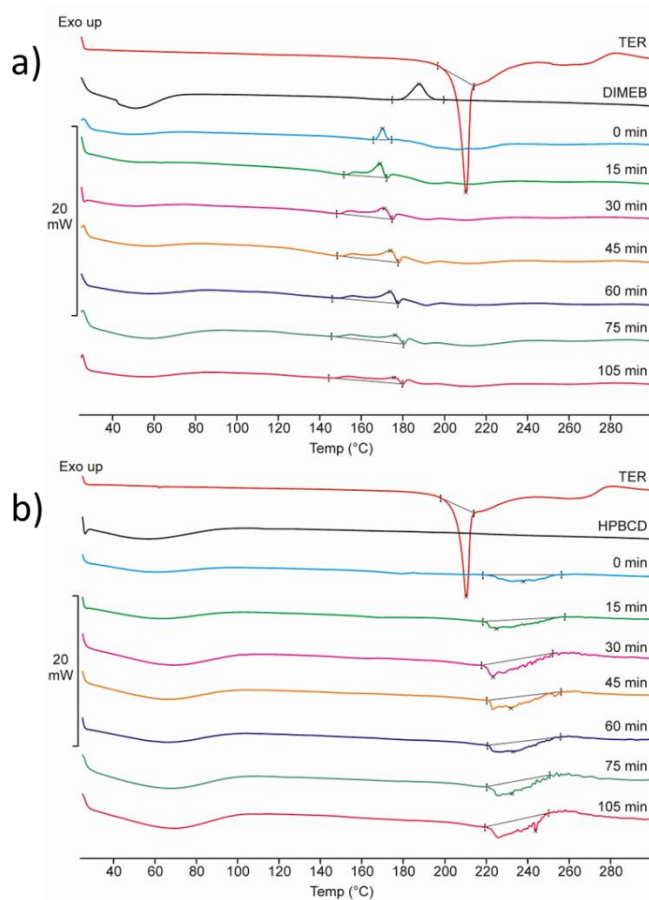


Figure 9. DSC thermograms of raw materials, PM (0 min), and products (15-105 min) containing DIMEB (a) and HPBCD (b).

5.2.2. Crystallographic characterization of binary systems of Terbinafine HCl

Only the XRPD diffractogram of TER exhibited distinct peaks, indicating crystallinity, while CDs, being amorphous materials, lacked well-defined peaks in their diffractograms. The peak intensity seen in the diffractogram of the PMs decreased as the grinding time progressed, and with 105 minutes of the process, the diffractograms exhibited the absence of well-defined peaks. The formation of amorphous character was observed with both CDs (Figure 10).

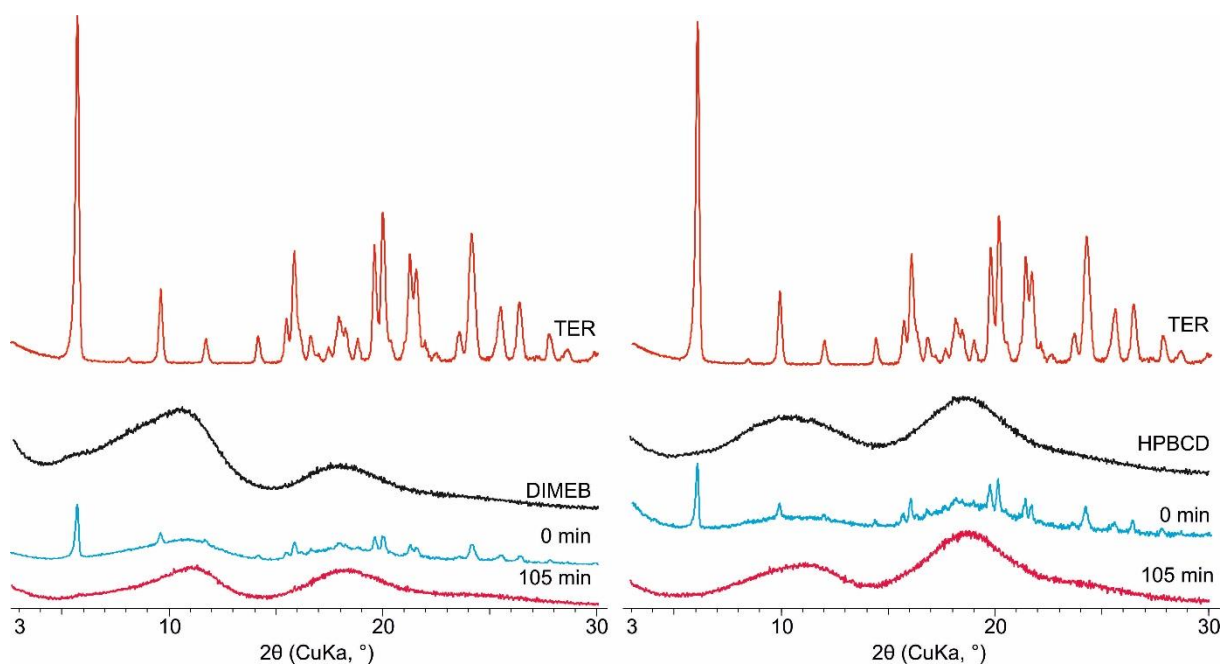


Figure 10. XRPD diffractograms of raw materials, PMs, and final CG products (105 min) containing DIMEB (a) and HPBCD (b).

5.2.3. Vibrational spectroscopic evaluation of binary systems of Terbinafine HCl

FTIR and Raman spectroscopy provide complementary information despite being based on the same set of normal vibrations. This is due to the distinct selection rules governing peak intensities in their spectra. The combination of these methods is particularly valuable for materials like TER, which contain both charged or highly polarized components and non-polar yet electron-rich elements such as multiple bonds and aromatic rings.

The infrared spectra of the samples, obtained at different grinding times, showed noticeable changes. The broad N-H stretching band of the ammonium group gradually diminished and became indistinguishable from the baseline after 30 minutes. Moreover, the characteristic bands of TER mostly vanished, became broader, and merged with the broad bands of the product, regardless of whether DIMEB or HPBCD was used. Among the spectral regions, the progress of product formation could be tracked for a longer duration in the out-of-plane vibrations of the aromatic rings between $820\text{-}675\text{ cm}^{-1}$ (Figure 11.).

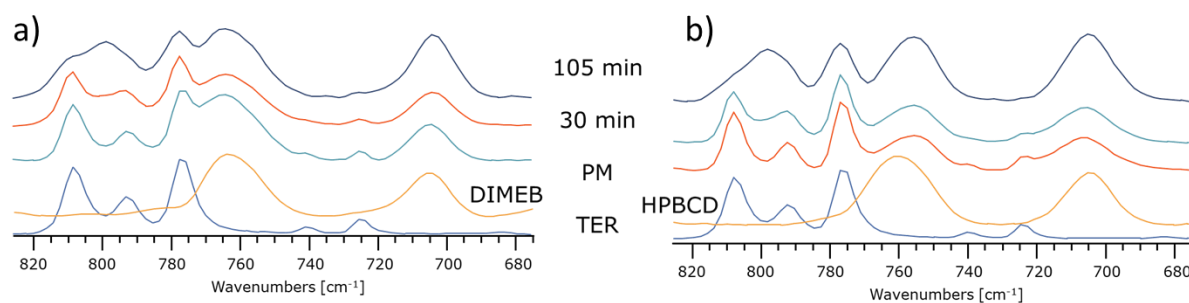


Figure 11. Selected spectra between 820-675 cm^{-1} FTIR spectra of the starting materials raw materials, PMs, an intermediate product (30 min), and final CG products (105 min) containing DIMEB (a) and HPBCD (b).

To monitor the component distribution in the sample, Raman intensity maps can be generated for various peaks. The effectiveness of this method relies on the careful selection of peaks for map construction. The TER's out-of-plane deformation modes of the aromatic rings and the stretching bands region of triple and double bonds seemed promising initially, but the products exhibited some intensities at those wavenumbers as well. There was a single peak at 1289.5 cm^{-1} in the challenging-to-assign fingerprint region, which proved to be useful in monitoring the presence and distribution of crystalline TER in the sample (Figure 12.a).

All samples were mapped using the 1289.5 cm^{-1} peak. It was observed that crystalline TER appeared as isolated "islands" in the samples during earlier stages of grinding, the disappearance of these signals confirmed the absence of crystalline TER in the samples after 75 minutes of grinding (Figure 12.b).

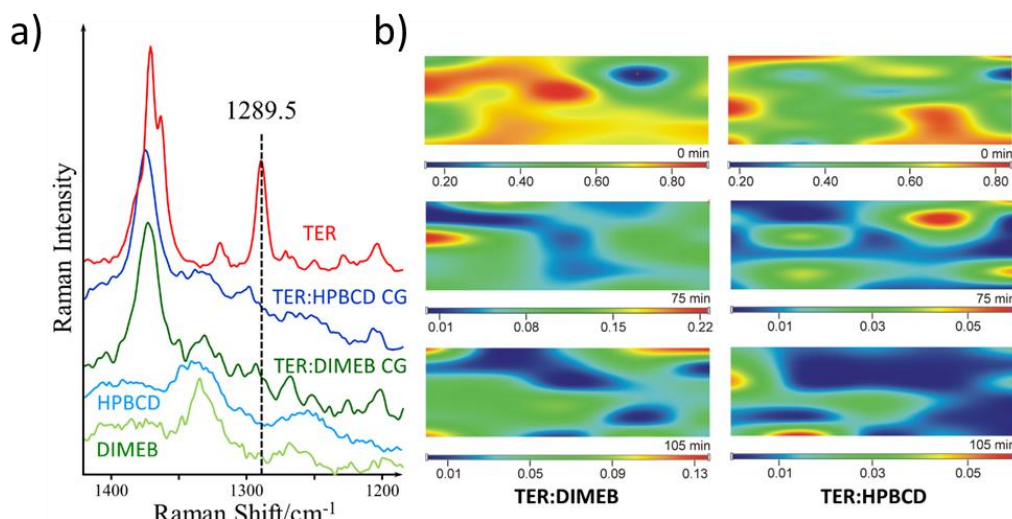


Figure 12. Raman region containing the peak at 1289.5 cm^{-1} for the characterization of the presence and the distribution of crystalline TER in the samples (a), and examples of Raman-intensity maps of the TER:DIMEB and the TER:HPBCD at 0, 75, and 105 min.

5.2.4. In vitro studies of binary systems of Terbinafine HCl

Dissolution studies were conducted using the paddle method with a reduced volume of dissolution medium. The dissolution profiles were graphed as the percentage of dissolved drug versus time.

The solubility of the TER is highly pH-dependent, with lower solubility observed at higher pH levels, resulting in incomplete dissolution or precipitation and reducing bioavailability. This can be a concern for TER, particularly at high doses. In SIF, the solubility of TER is below 1%. The use of CDs demonstrated a solubility-enhancing effect on TER. However, the extent of this enhancement varied depending on the CD used. The TER product containing DIMEB showed a significant increase in DE to $4.81 \pm 0.09\%$ by 120 minutes, and a higher dissolution rate indicated by the MDT value. On the other hand, the HPBCD product exhibited a lesser increase in DE to $1.70 \pm 0.02\%$, accompanied by a lower dissolution rate compared to the pure drug (Table 5). In SGF, the solubility of TER reached nearly 100%. Both CD had a positive impact in this scenario, enhancing the dissolution rate of the API as evidenced by the decreased MDT values (Table 5).

Table 5. DE and MDT values in SIF and SGF.

	Simulated intestinal medium			Simulated gastric medium		
	DE _{60min}	DE _{120min}	MDT	DE _{60min}	DE _{120min}	MDT
TER	0.85±0.05	0.90±0.04	18.88±7.49	68.57±6.91	80.45±5.19	18.35±2.69
TER:DIMEB	4.75±0.09	4.81±0.09	11.02±2.00	88.68±1.50	91.54±1.02	12.54±6.08
TER:HPBCD	1.40±0.04	1.70±0.02	28.86±1.63	88.80±0.84	88.54±1.32	7.69±5.68

5.3 Ternary systems of Terbinafine HCl with cyclodextrins and water-soluble polymers

The TER:SBEB CD:PVP (TSP) and the TER:SBEB CD:HPMC (TSH) products obtained by different methods have been prepared and evaluated in this part. The 2 polymers were used in 5 and 15 w/w%, and the 3 methods were applied for all compositions. As a combination of these compositions and methods, 15 products were prepared.

Table 6. Abbreviations of products based on materials and preparation methods.

Abbreviation	Methods	Materials	Percentage of polymer (%)
TS SE	Solvent evaporation		
TS KN	Kneading	TER,	0
TS CG	Co-grinding	SBEB CD,	
TSP SE 5%			5
TSP SE 15%	Solvent evaporation		15
TSP KN 5%		TER,	5
TSP KN 15%	Kneading	SBEB CD,	15
TSP CG 5%		PVP	5
TSP CG 15%	Co-grinding		15
TSH SE 5%			5
TSH SE 15%	Solvent evaporation		15
TSH KN 5%		TER,	5
TSH KN 15%	Kneading	SBEB CD,	15
TSH CG 5%		HPMC	5
TSH CG 15%	Co-grinding		15

5.3.1. Thermoanalytical characterization of ternary systems of Terbinafine HCl

The thermal curves of individual components, their PM, and presumed inclusion complexes reveal changes in solid-state and component interactions, influenced by the methods used to form ternary systems. DSC data (Figure 13.a) displayed a distinct peak at approximately 209 ± 0.2 °C for TER, followed by decomposition at higher temperatures. The DSC curve of SBEB CD demonstrated the amorphous nature of the CD derivative, characterized by a broad and intense endothermic effect with a peak around 90–100 °C, representing dehydration, followed by decomposition above 280 °C. PVP exhibited a significant endotherm peak between 40 and 110 °C, indicating water loss. HPMC exhibited a similar thermal profile, with a broad endothermic transition around 60 °C.

The DSC curves of different samples showed disappearance of the melting peak, indicating partial loss of TER crystallinity due to solid-state interactions between components. TG measurements were also investigated to analyse the thermoanalytical behavior of the materials and gain insights into the observed decomposition in the DSC measurements. Each product exhibited multiple stages of mass loss. The first derivative of the TG curves was calculated and presented alongside the TG and DSC curves to facilitate the identification of each inflection point. Figure 13.b illustrates the recorded DSC, TG, and 1st derivative of the TG curves for TSH CG 5%, which serves as a representative sample of all prepared ternary systems.

The first weight losses observed at the beginning of the TG curves for all products correspond to the detection of the original water content present in the CD. Subsequent mass decreases observed in the curves indicate the degradation of compounds, which is consistent with the prolonged complex phenomenon observed in the DSC curves. The disappearance of the melting point of the crystalline drug in the DSC curves of the presumed complexes provides evidence of the drug molecule being incorporated into the CD cavity.

Furthermore, comparing the TG curves of pure TER with those of the ternary systems, it was observed that the decomposition occurred within the same temperature range. This suggests that the products did not enhance the thermal stability of the API.

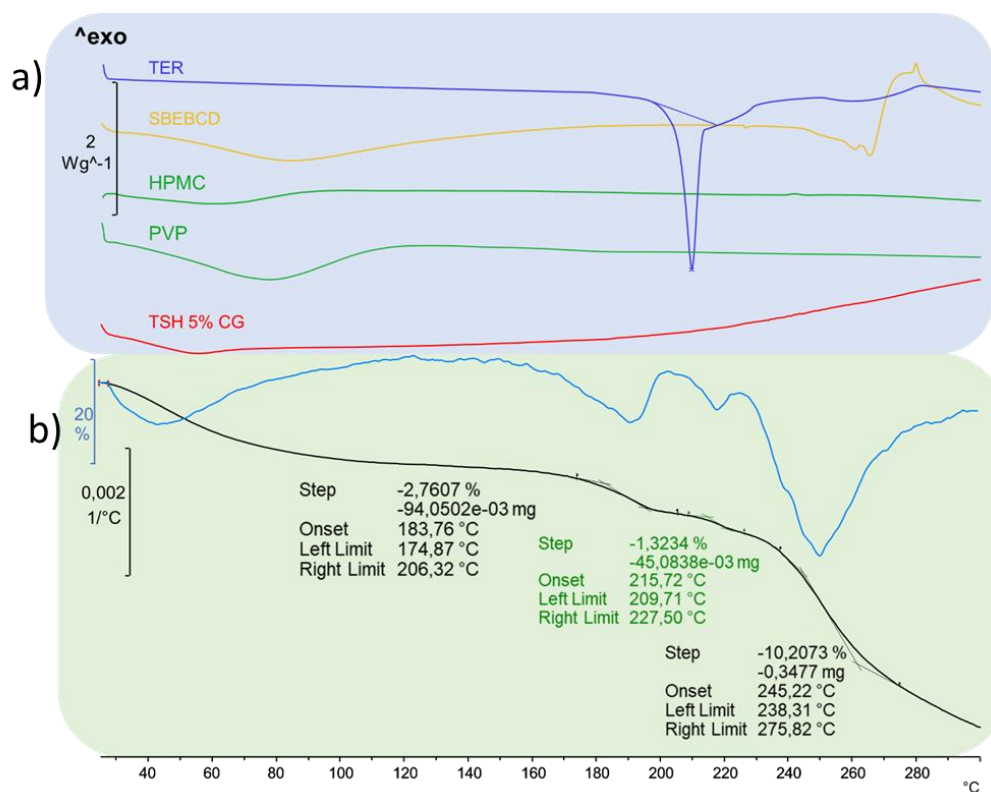


Figure 13. DSC thermograms of starting materials and TSH CG 5% as a representation of all amorphous products (a). TG, and 1st derivative of the TG curves for TSH CG 5% (b).

5.3.2. Crystallographic characterization of ternary systems of Terbinafine HCl

XRPD patterns on the powder of the individual components and the products were compared. The preparation methods of the complexes using SE and CG resulted in amorphous products with both polymers. However, the obtained products using the KN exhibited characteristic peaks of TER, indicating only partial loss of crystallinity. Generally, the percentage of polymer used did not influence the crystalline nature of the products.

Amorphization of the products was achieved through the continuous energy supply during the grinding process. Increasing the grinding time led to a greater loss of crystallinity, with the characteristic peaks of the drug showing decreased intensity. For example, the product containing 5 w/w% PVP required 70 minutes of grinding for complete amorphization, while all other products achieved it in a shorter time of 30 minutes. This behavior was observed across all systems, regardless of the polymer used in the preparation of the ternary system (Figure 14). Notably, applying the same grinding procedure for pure TER for the longest time (70 minutes) did not result in the amorphization of the API.

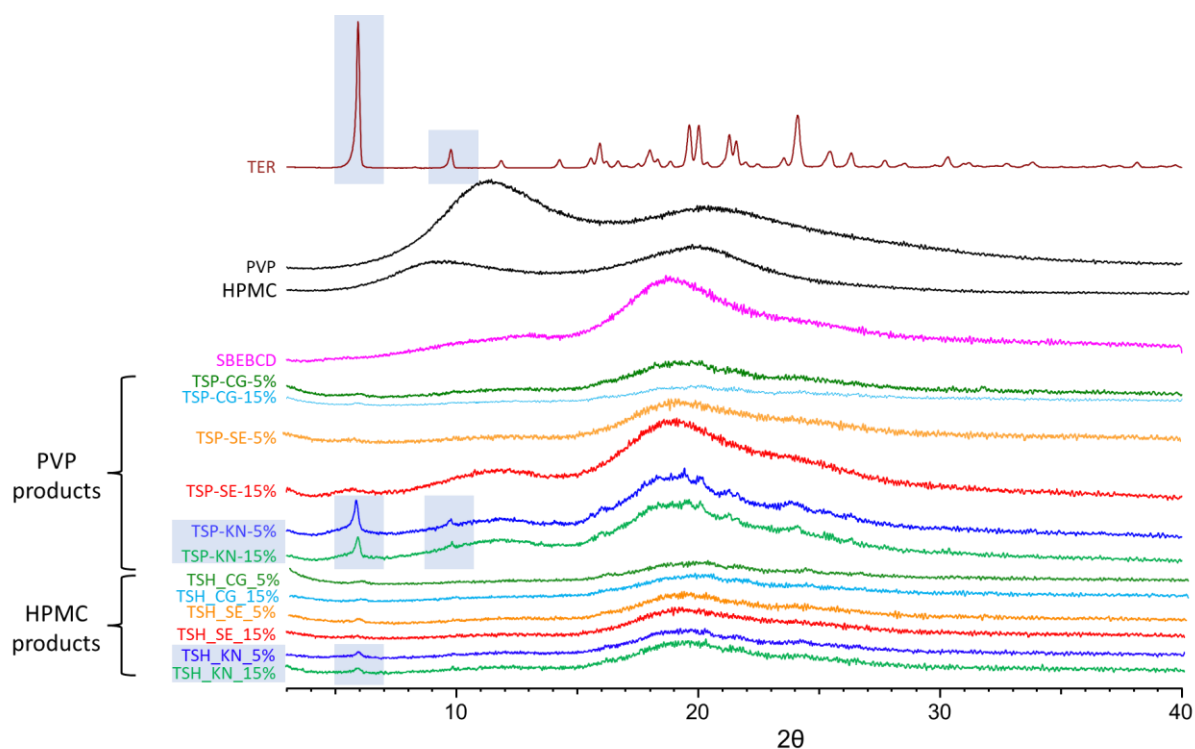


Figure 14. XRPD diffractograms of raw materials and all products. Crystalline peaks were highlighted in the case of TER and KNs.

To further examine the changes in crystalline properties induced by grinding and assess the influence of polymers on grinding time, mechanochemical activation was performed using a milling machine while maintaining the same material composition. The initial degree of crystallinity was approximately 16%, considering that the starting PM also contained a significant amount of amorphous material due to the presence of excipients, resulting in an amorphous background in the diffractograms. Plotting the crystallinity against grinding time revealed similar curves for all products. For all product he most significant decrease in crystallinity occurred within the first two minutes, reaching the minimum detectable crystallinity by the instrument within 12 minutes (Figure 15.).

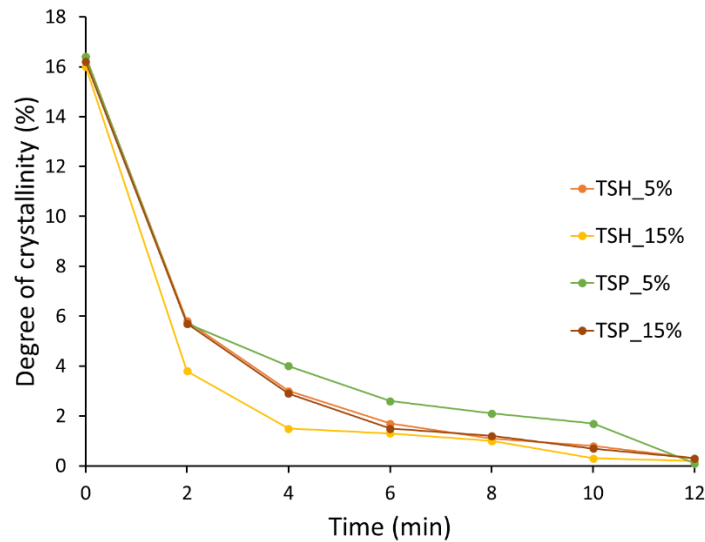


Figure 15. Percentage of the crystalline material of milled samples as a function of time.

SEM analysis was performed on TER and the products obtained through various techniques, with a focus on samples containing 5% of the polymer (presented in Figure 16.). TER crystals appeared as aggregates, exhibiting a flat crystalline profile with an average diameter of $15.904 \pm 7.090 \mu\text{m}$. The crystal surface was smooth, with rounded edges and no cracks. The SE method resulted in smooth-surfaced samples, with small sections of polymer film-like cohesive material forming a film in the case of HPMC. Samples containing PVP showed larger crystals with smooth surfaces and sharp edges.

The SE method yielded uncertain results in terms of particle size. The average diameter for the sample obtained with PVP was $21.408 \pm 14.791 \mu\text{m}$, while for HPMC it was $8.122 \pm 3.279 \mu\text{m}$. Notably, using PVP as the polymer resulted in significantly larger particle sizes compared to all other samples except for TSP CG, with a significant difference ($p < 0.01$). There was also a significant difference ($p < 0.05$) in size compared to TER. Evaporation of the solvent method was not desirable for achieving controlled particle diameter, making it not recommended for product manufacturing.

Using the KN preparation method, there was no significant difference in the particle size of the samples prepared with the two polymers. The particle size was $14.924 \pm 7.110 \mu\text{m}$ for PVP products and $14.869 \pm 5.224 \mu\text{m}$ for HPMC products. SEM images showed a strong similarity, with particles having small, irregular, and flat morphology.

Similarly, the particle size of the samples produced by CG was not influenced by the polymer used. Both PVP and HPMC CG products exhibited a size similar to that of untreated TER crystals. The particle size was $17.813 \pm 8.157 \mu\text{m}$ for products with PVP and

$15.178 \pm 7.441 \mu\text{m}$ for products with HPMC. A notable difference was that the grinding process made the particles rough and wrinkled instead of smooth. Additionally, the particles had an irregular shape in this case.

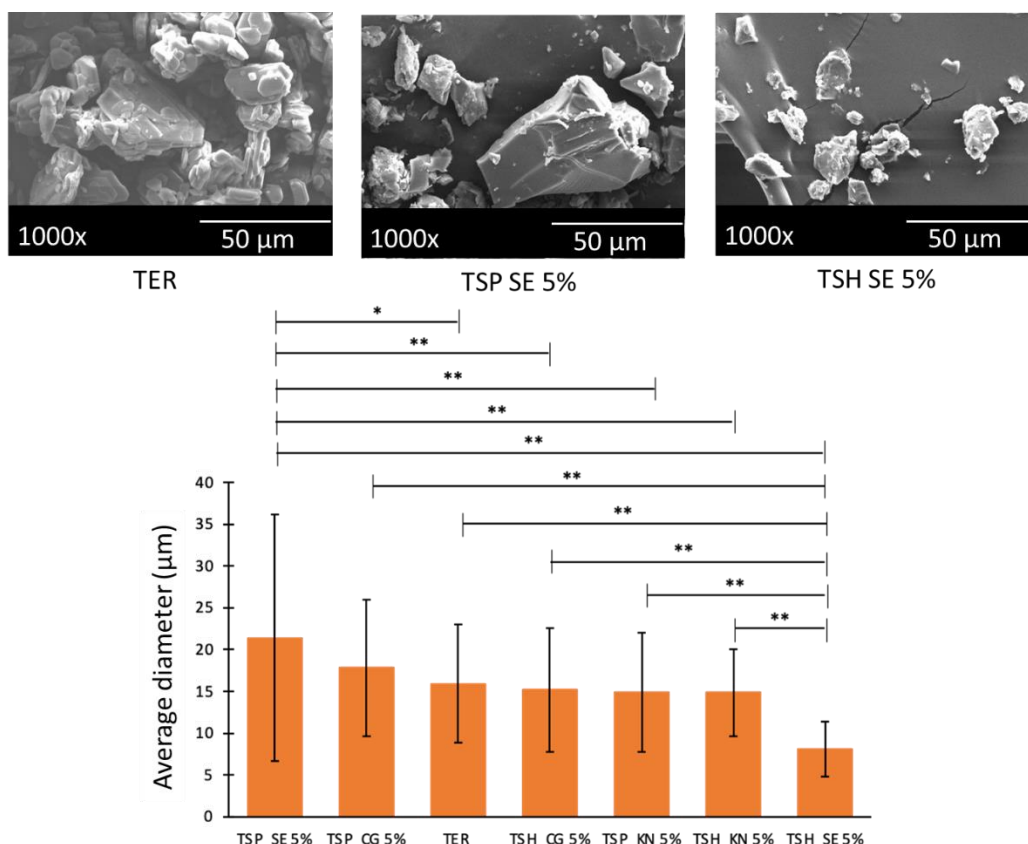


Figure 16. SEM images (up) of TER and SE products. Average diameter (down) of products containing 5% of the polymer. Experimental results with p-values <0.05 (*) and <0.01 (**) were assumed to be statistically significant.

5.3.3. Vibrational spectroscopic evaluation of ternary systems of Terbinafine HCl

The FTIR analysis provided additional insights into the intermolecular interactions between TER and the excipients. The TER spectrum exhibited characteristic and intense bands at 2968, 2446, 1361, 1631, 1514, 958, 1450, 1318, and 1248 cm^{-1} , along with three bands in the range of 820-760 cm^{-1} .

In the CG products, a broad band corresponding to the amine group at 2446 cm^{-1} was present, which disappeared in SE and KP products (Figure 17.a). The aromatic out-of-plane bands (in the range of 820-760 cm^{-1}) and the aromatic C=C bond band (1514 cm^{-1}) did not exhibit any shifting or decrease in intensity. The band related to the aliphatic C=C group (1631 cm^{-1}) was not detectable in the products due to the presence of a broad band attributed to the

CD in the same region. The trans-substituted olefin group band at 958 cm^{-1} was only detected in the CG products, although reduced and shifted (Figure 17.b). Other C=C bands associated with stretching vibration at 1450 , 1318 , and 1248 cm^{-1} either completely disappeared or, in the case of CG products with HPMC, significantly reduced and shifted (Figure 17.c). However, for PVP, interpreting interactions using the band at 1318 cm^{-1} was challenging due to the presence of a broad band in this spectral range associated with PVP itself.

There are some differences in spectral changes depending on the polymer used. For aromatic C-H deformation bands referring to the methyl and methylene groups at 2968 cm^{-1} disappearance of the peak can be seen in the spectra of TSP SE products and shifting in TSP KP and CG products, while there were no changes in the spectra of HPMC-products. Similarly, shifting of t-butyl axial deformation (1361 cm^{-1}) can be detected in all PVP products, in HPMC KP and CG products no changes occurred, except for shifting bands of TSH SE products.

Overall, the amount of polymers used did not affect the interactions that occurred, so for better transparency, only products containing 5% of polymer are shown in Figure 17.

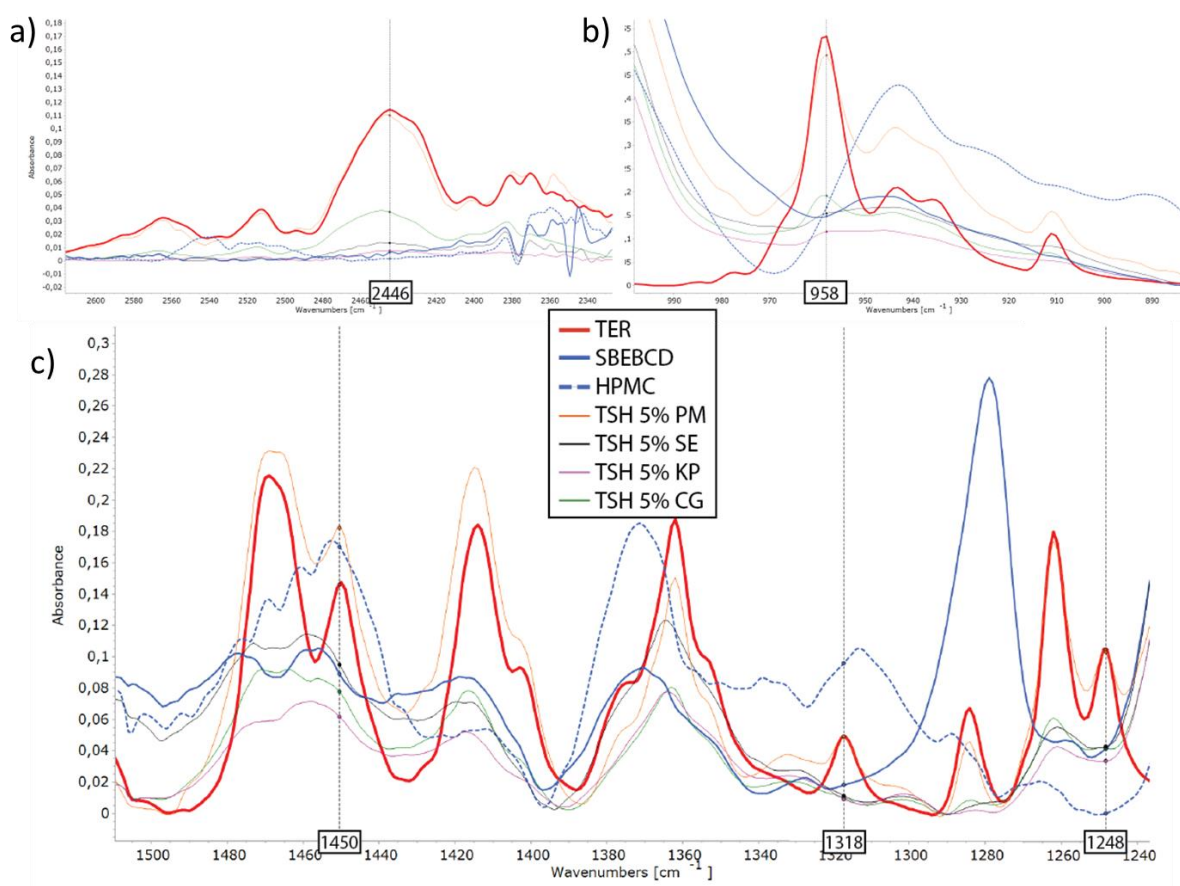


Figure 17. Selected regions of FTIR spectra of TSH products and corresponding raw materials and their PM. Amine group at 2446 cm^{-1} (a), trans-substituted olefin group band at 958 cm^{-1} (b), C=C bands associated with stretching vibration at 1450 , 1318 , and 1248 cm^{-1} (c).

Physicochemical characterization showed no difference between products with 5% and 15% polymers, so further tests were carried out with 5% polymer-containing products.

5.3.4. In vitro studies of ternary systems of Terbinafine HCl

In vitro dissolution studies were performed to assess the dissolution performance of the formulations in comparison to the pure drug, binary system, and pulverised commercial product Terbisil® tablet. Various pH conditions were tested in the dissolution studies to comprehensively understand the release profiles of TER. In the SIM dissolution experiments, the DE was calculated at 120 minutes (Figure 18.). Pure drugs and Terbisil® exhibited DE of less than 1%, which increased to around 8% when using SBEB CD alone. PVP products did not further enhance the DE, indicating no impact of this polymer on solubility improvement.

However, HPMC products approximately doubled the DE, with variations among the different products. Among them, CG products showed the highest DE value, reaching approximately 20%.

In lower pH, in the SGM dissolution of TER results in increased dissolution. Over 90% of the pure drug dissolves within 60 minutes. However, the products achieve this level of dissolution in a shorter time, indicating a higher dissolution rate. To measure this phenomenon, the MDT was calculated (Figure 18.). A lower value of MDT means a faster dissolution rate. The MDT reveals a longer dissolution time for TER compared to each product, including the pulverised marketed product. However, none of the products exhibit a significantly lower MDT than the binary system.

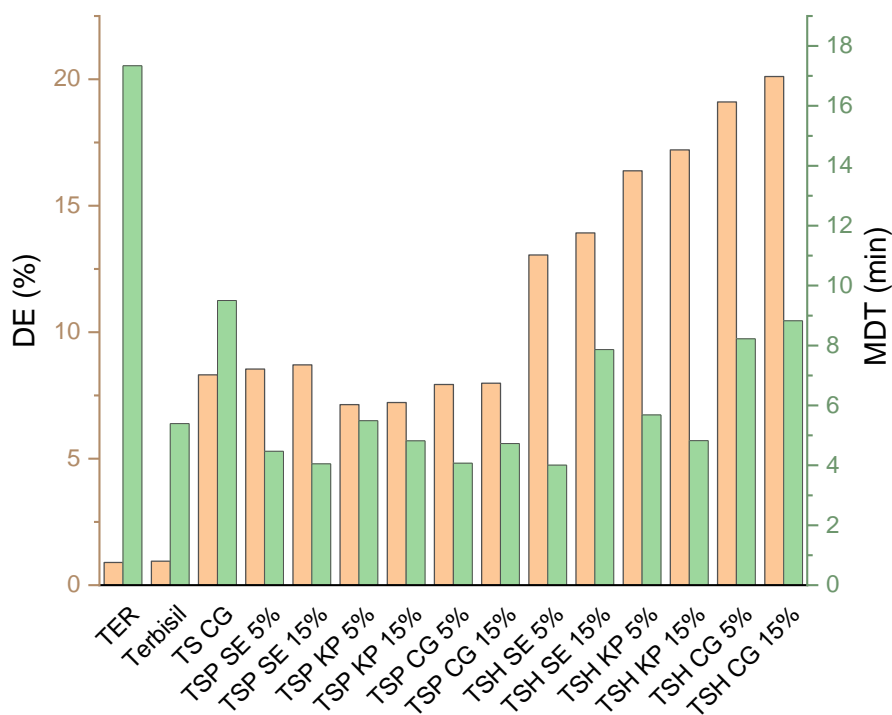


Figure 18. DE values at 120 minutes were measured in SGF and MDT values were measured in SIF.

Cytotoxicity studies were conducted for samples containing 5% polymer. MTT assay studies were performed to evaluate the impact of the products and the TER on cell viability. The tests included pure TER, SBEB CD, and ternary products. Concentrations of TER and the products were applied at a serial two-fold dilution of 1 mg/mL TER concentration. The concentration of SBEB CD was diluted serially at a two-fold concentration of 4.89 mg/mL.

SBEBBCD exhibited the least cell toxicity among the tested samples, marked with blue in Figure 19. Only the highest concentration sample (4.89 mg/mL) demonstrated reduced cell viability, while all other dilutions remained within the non-toxic range.

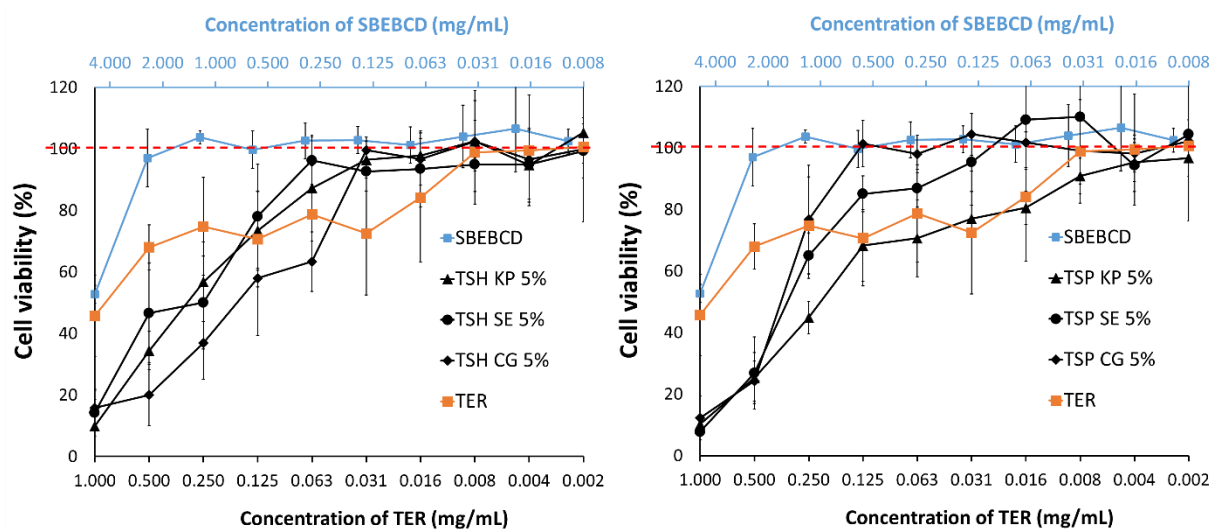


Figure 19. Cell viability (%) as a relationship between TER concentration (lower x-axis) and SBEBBCD concentration (upper x-axis) in reverse order on a logarithmic two scale. The two raw materials are shown in both graphs. Products with PVP (a) and HPMC (b) showed in black since those were depicted as their TER-content concentration. 100 % of cell viability was marked with the red dashed line, as a marker of non-toxic level.

At a concentration of 1 mg/mL, pure TER (marked with orange in Figure 19.) exhibited 45.66% (± 13.21) cell viability. However, the cell viability of all products was lower than that of pure TER at this concentration. When pure TER was diluted, cell viability remained within the toxic range until a dilution of 0.008 mg/mL. In contrast, the products showed reduced cell toxicity as they reached the non-toxic level at higher concentrations of TER, ranging from 0.125 to 0.31 mg/mL. The only exception was TSP KP 5%, where the highest non-toxic concentration was 0.004 mg/mL, suggesting poorer cell viability properties.

5.4 Stability tests of prepared co-ground products

We have shown above that inclusion complexes were formed during CG with the applied substances and that the properties of the APIs were modified. One of the most important of these changes was the formation of amorphous products from crystalline APIs. Since such products are prone to recrystallization over time, stability studies were performed. DIMEB complexes of the two tested drugs were selected from the previous products prepared by CD

grinding. Stability studies were performed for 3 months under normal conditions at room temperature and accelerated stability studies at higher temperatures and humidity (40 °C and relative humidity of 75%). The amorphous properties were most effectively monitored by DSC and XRPD measurements.

5.4.1. Thermoanalytical characterization during stability tests

For the freshly prepared samples, the DSC thermograms did not contain a peak characteristic of the APIs for either drug. However, they did both contain an endothermic broadening peak due to the water content of the product at low temperatures. Furthermore, both thermograms (Figure 20.) show an exothermic peak indicative of the recrystallization of a substance. These exothermic peaks appeared at different temperature values (100 °C for FEN and 151 °C for TER). The recrystallized materials melted in a temperature range close to each other (185 °C for FEN and 195 °C for TER). This indicates that it's likely that the same crystal was formed during the previous recrystallization but at different temperatures depending on the product.

The TER product retained its thermal properties during this period in both the normal and accelerated stability tests. Therefore, from these data, it appears to be a stable amorphous product. Only a slight shift of recrystallized material's melting point can be observed. For FEN, as for TER, there was no change in the stability tests under normal conditions, with similar thermograms after 3 months as for the freshly prepared sample. The difference between the two products was between the values measured in the accelerated stability test at 3 months. Under these conditions, the product containing FEN no longer retained its original thermal behaviour. A melting point of around 80 °C, typical of the original API, was observed, suggesting that the original polymorph of FEN was present in crystalline form in some quantity. Furthermore, the previously observed exothermic peak was not detected, but, controversially, the melting point indicative of the recrystallized product was unchanged. To investigate this apparent contradiction, XRPD studies were performed at room temperature and gradually increased temperature.

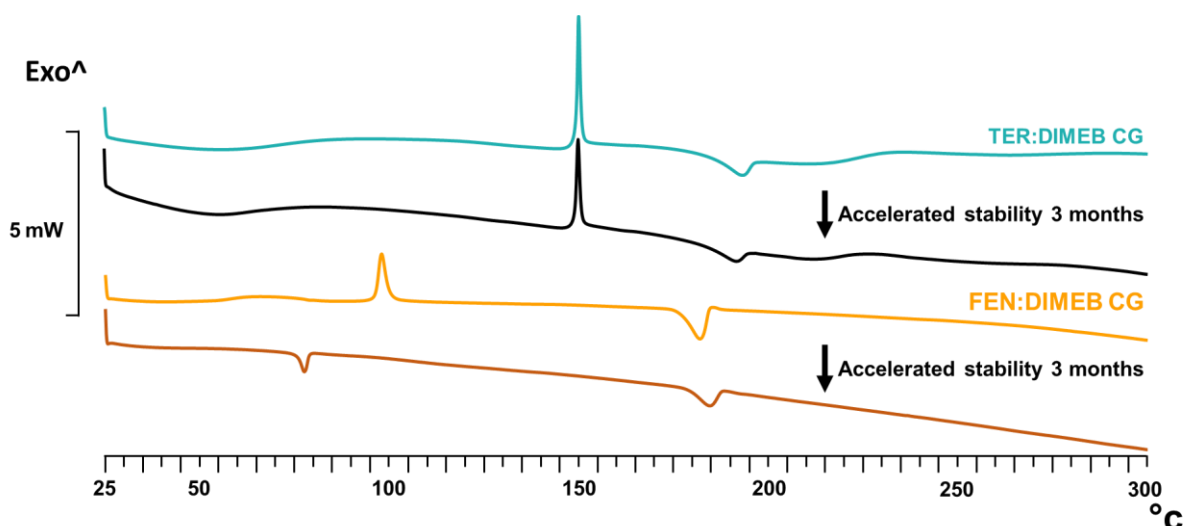


Figure 20. DSC thermograms of CG products and corresponding data of samples after 3 months accelerated stability test.

5.4.2. Crystallographic characterization during stability tests

The Figure 21. shows the diffractograms of the APIs used, the freshly prepared CG products, and the samples of 3-month accelerated stability tests. Also shown are the diffractograms selected from HOT-XRPD measurements at different temperatures for the two products, corresponding to the exothermic peak temperatures seen in the DSC thermograms.

In the case of TER, we also found during XRPD tests that the physicochemical properties of the product did not change either under normal or elevated conditions during 3 months. The diffractograms of the product show that the products are amorphous, the characteristic peaks of TER are not present, and this property does not change during the stability tests. HOT-XRPD measurements demonstrate the crystallization of a material at 175 °C that is different from the original TER crystal structure and all known polymorphic crystal structures of TER.

The stable amorphous form was also characteristic of the FEN product during the tests carried out under normal conditions. However, during accelerated tests, the initially amorphous product showed crystalline peaks that were different from those of the original FEN and every known polymorph of the API. The peaks characteristic of FEN can only be observed to a small extent, but the determination of this is disturbed by the presence of the unknown, recrystallized material.

In accordance with the exothermic peak on the DSC thermograms, this time around 105 °C we could also experience the appearance of crystalline material during HOT-XRPD

measurements. The crystallized material showed the same peaks that were observed in the accelerated stability test of the FEN product. This resolves the apparent contradiction we raised with DSC measurements. Because the product did not have to recrystallize during the DSC measurements, it was already present in the product at room temperature. Furthermore, it can be observed that the product recrystallized in the case of TER also shows the same peaks.

The differences observed during the accelerated stability tests of the two products may be because the temperature required for recrystallization of the FEN product is very close to the temperature used during the accelerated stability test. Since the product was exposed to this slightly lower temperature for a longer time than during the DSC measurements, it received a higher thermal load, so it recrystallized even at a lower temperature. However, this temperature was not sufficient for the recrystallization at a temperature higher than the TER during the test.

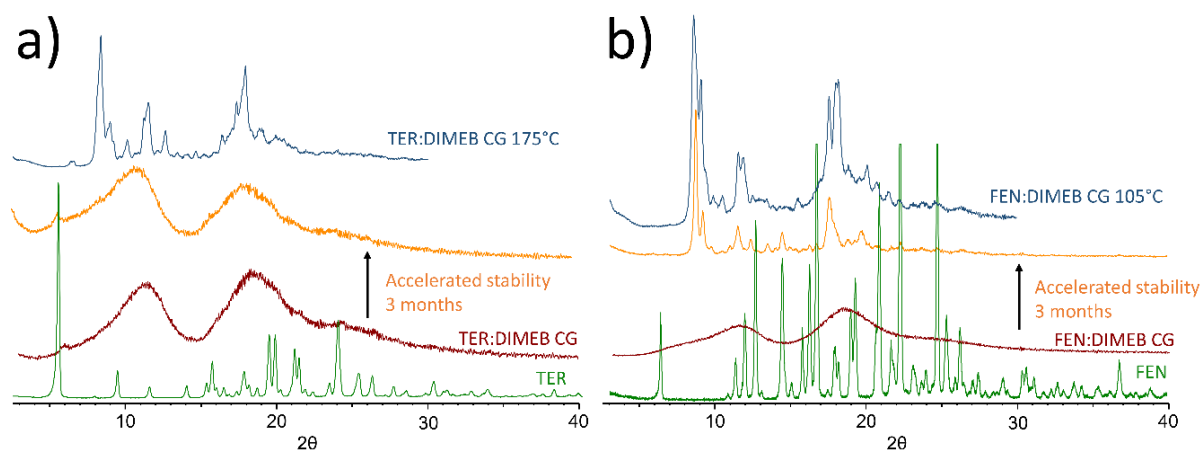


Figure 21. Diffractograms of the APIs (TER: left, FEN: right) used the freshly prepared CG products, the samples of 3-month accelerated stability tests. Upper diffractograms shows HOT-XRPD measurements on different temperature.

We can conclude that based on both DSC and XRPD measurements the TER product has stable amorphous properties, while the FEN products are less stable at high temperatures and humidity due to the low-temperature crystallization process.

6. CONCLUSION

The novel results of this Ph.D. work aim to prepare CD complexes in the novel, solventless method and compare conventional methods, that is summarized in the following points:

I) During this work co-ground CD complexes were prepared using FEN and TER. CD complexation is a widely studied area of pharmaceutical technology. However, despite the advantages of the method, there are only a few studies dealing with solventless, CG complexation.

II) FEN complexes were prepared with DIMEB. Based on the DSC thermograms, the disappearance of the melting point associated with the API indicates the presence of amorphous properties. This finding was further supported by the XRPD measurements, which revealed the formation of amorphous products via grinding, while KN produced a crystalline and amorphous mixture. Changes in the FTIR spectra indicated a three-stage process, proving the fact of complexation. Dissolution studies showed increased DE for the products. Based on these findings, XRPD and DSC studies can be useful in monitoring the degree of complexation during grinding when intermolecular interactions between materials have been characterized using other methods.

III) TER-containing CD complexes were successfully prepared by grinding API and two kinds of CD derivatives. The DSC thermograms do not show the characteristic melting point of the drug, suggesting interactions between the components. The XRPD measurements also showed that the formation of presumed complexes is a time-consuming process leading to practically amorphous products. FTIR results confirmed that TER with DIMEB or HPBCD formed an inclusion complex through the unsaturated alkyl-chain of TER by simple grinding. A peak in Raman spectra was found at 1289.5 cm^{-1} characteristic of the crystalline form of TER used to construct Raman microscopic images to follow the distribution of the unreacted TER in the samples. Dissolution studies showed that each product has a higher dissolution rate in both applied mediums and that each product has a higher solubility than the API in SIF.

IV) Complexation of TER with SBEB CD and the modifying effects of two different polymers, PVP and HPMC were investigated. Two concentrations of the polymers, 5, and 15 w/w%, were used. The ternary complexes were compared with the binary complex, drug alone, and commercial tablet formulation of TER. FTIR measurements showed that different

methods of obtaining ternary complexes and different polymer excipients had varying effects on the non-covalent bond formation between the drug and CD. These interactions influenced thermoanalytical and in vitro behaviors. Overall, both polymers positively modified the complex properties, with no significant difference observed between the polymer concentrations used. The 5 w/w% systems exhibited similar synergistic effects and did not affect the trend of crystallinity decrease compared to the 15 w/w% systems. This suggests that a lower polymer concentration is sufficient to achieve the same effect. Additionally, the 15 w/w% polymer product contained a lower CD concentration, which has economic advantages. By adding a larger amount of cheaper polymer, the relatively expensive CD derivative, and API can be reduced. These findings indicate that polymers can enhance bioavailability and should be considered in a future product design of these materials, taking into account the lower material cost associated with producing complexes.

V) During real-time stability studies no changes were observed in the thermoanalytical and crystalline properties of the products. Similar phenomena were observed for TER in the accelerated stability tests. However, the FEN products showed crystalline properties under these conditions. However, this crystallized material did not match the initial FEN or any polymorphs of FEN.

The main new findings and practical aspects of the work:

1. FEN complexes with DIMEB were prepared via CG for the very first time, with a comprehensive analytical evaluation.
2. For the first time, binary complexes of TER with DIMEB and HPBCD were prepared using the CG technique, and a comprehensive analytical evaluation was performed.
3. Using the CG technique, ternary complexes of TER with SBEB CD and polymers (PVP and HPMC) were successfully prepared for the first time, followed by a comprehensive analytical evaluation.
4. We utilized a range of analytical methods to assess the CG method and establish a rapid screening protocol essential for the CG procedure with CD binary and ternary systems.
5. However, applied APIs were model drugs, with improved physicochemical properties suggesting possible “Supergenerics” can be formulated in the future.

REFERENCES

- [1] K.T. Savjani, A.K. Gajjar, J.K. Savjani, Drug Solubility: Importance and Enhancement Techniques, *ISRN Pharmaceutics*. 2012 (2012) 1–10. <https://doi.org/10.5402/2012/195727>.
- [2] G.L. Amidon, A Theoretical Basis for a Biopharmaceutic Drug Classification: The Correlation of in Vitro Drug Product Dissolution and in Vivo Bioavailability, *Pharm. Res.* 12 (1995) 413–420.
- [3] M. Lindenberg, S. Kopp, J.B. Dressman, Classification of orally administered drugs on the World Health Organization Model list of Essential Medicines according to the biopharmaceutics classification system, *European Journal of Pharmaceutics and Biopharmaceutics*. 58 (2004) 265–278. <https://doi.org/10.1016/j.ejpb.2004.03.001>.
- [4] Y. Kawabata, K. Wada, M. Nakatani, S. Yamada, S. Onoue, Formulation design for poorly water-soluble drugs based on biopharmaceutics classification system: Basic approaches and practical applications, *International Journal of Pharmaceutics*. 420 (2011) 1–10. <https://doi.org/10.1016/j.ijpharm.2011.08.032>.
- [5] D.V. Bhalani, B. Nutan, A. Kumar, A.K. Singh Chandel, Bioavailability Enhancement Techniques for Poorly Aqueous Soluble Drugs and Therapeutics, *Biomedicines*. 10 (2022) 2055. <https://doi.org/10.3390/biomedicines10092055>.
- [6] P. Anastas, N. Eghbali, Green Chemistry: Principles and Practice, *Chem. Soc. Rev.* 39 (2010) 301–312. <https://doi.org/10.1039/B918763B>.
- [7] P.T. Anastas, J.C. Warner, Green chemistry: theory and practice, Oxford University Press, Oxford [England] ; New York, 1998.
- [8] J.B. Zimmerman, P.T. Anastas, H.C. Erythropel, W. Leitner, Designing for a green chemistry future, *Science*. 367 (2020) 397–400. <https://doi.org/10.1126/science.aay3060>.
- [9] K.J. Ardila-Fierro, J.G. Hernández, Sustainability Assessment of Mechanochemistry by Using the Twelve Principles of Green Chemistry, *ChemSusChem*. 14 (2021) 2145–2162. <https://doi.org/10.1002/cssc.202100478>.
- [10] J. Becker, C. Manske, S. Randl, Green chemistry and sustainability metrics in the pharmaceutical manufacturing sector, *Current Opinion in Green and Sustainable Chemistry*. 33 (2022) 100562. <https://doi.org/10.1016/j.cogsc.2021.100562>.
- [11] B.W. Cue, J. Zhang, Green process chemistry in the pharmaceutical industry, *Green Chemistry Letters and Reviews*. 2 (2009) 193–211. <https://doi.org/10.1080/17518250903258150>.
- [12] D.J.C. Constable, A.D. Curzons, V.L. Cunningham, Metrics to 'green' chemistry—which are the best?, *Green Chem.* 4 (2002) 521–527. <https://doi.org/10.1039/B206169B>.
- [13] D.J.C. Constable, C. Jimenez-Gonzalez, R.K. Henderson, Perspective on Solvent Use in the Pharmaceutical Industry, *Org. Process Res. Dev.* 11 (2007) 133–137. <https://doi.org/10.1021/op060170h>.
- [14] O.V. Kharissova, B.I. Kharisov, C.M. Oliva González, Y.P. Méndez, I. López, Greener synthesis of chemical compounds and materials, *R. Soc. Open Sci.* 6 (2019) 191378. <https://doi.org/10.1098/rsos.191378>.
- [15] S.A. Ross, D.A. Lamprou, D. Douroumis, Engineering and manufacturing of pharmaceutical co-crystals: a review of solvent-free manufacturing technologies, *Chem. Commun.* 52 (2016) 8772–8786. <https://doi.org/10.1039/C6CC01289B>.
- [16] K. Grodowska, A. Parczewski, ORGANIC SOLVENTS IN THE PHARMACEUTICAL INDUSTRY, (n.d.) 11.
- [17] European Medicines Agency, ICH Q3C (R8) Residual Solvents, <https://www.ema.europa.eu/en/ich-q3c-r8-residual-solvents> (accessed on 12 Aug 2023).

- [18] X. Liu, Y. Li, L. Zeng, X. Li, N. Chen, S. Bai, H. He, Q. Wang, C. Zhang, A Review on Mechanochemistry: Approaching Advanced Energy Materials with Greener Force, *Advanced Materials*. 34 (2022) 2108327. <https://doi.org/10.1002/adma.202108327>.
- [19] S. Pagola, Outstanding Advantages, Current Drawbacks, and Significant Recent Developments in Mechanochemistry: A Perspective View, *Crystals*. 13 (2023) 124. <https://doi.org/10.3390/cryst13010124>.
- [20] M. Solares-Briones, G. Coyote-Dotor, J.C. Páez-Franco, M.R. Zermeño-Ortega, C.M. de la O Contreras, D. Canseco-González, A. Avila-Sorrosa, D. Morales-Morales, J.M. Germán-Acacio, Mechanochemistry: A Green Approach in the Preparation of Pharmaceutical Cocrystals, *Pharmaceutics*. 13 (2021) 790. <https://doi.org/10.3390/pharmaceutics13060790>.
- [21] A. Stolle, R. Schmidt, K. Jacob, Scale-up of organic reactions in ball mills: process intensification with regard to energy efficiency and economy of scale, *Faraday Discuss*. 170 (2014) 267–286. <https://doi.org/10.1039/C3FD00144J>.
- [22] D. Hasa, W. Jones, Screening for new pharmaceutical solid forms using mechanochemistry: A practical guide, *Advanced Drug Delivery Reviews*. 117 (2017) 147–161. <https://doi.org/10.1016/j.addr.2017.05.001>.
- [23] M. Ferguson, N. Giri, X. Huang, D. Apperley, S.L. James, One-pot two-step mechanochemical synthesis: ligand and complex preparation without isolating intermediates, *Green Chem*. 16 (2014) 1374–1382. <https://doi.org/10.1039/C3GC42141D>.
- [24] F. Schneider, T. Szuppa, A. Stolle, B. Ondruschka, H. Hopf, Energetic assessment of the Suzuki–Miyaura reaction: a curtate life cycle assessment as an easily understandable and applicable tool for reaction optimization, *Green Chem*. 11 (2009) 1894. <https://doi.org/10.1039/b915744c>.
- [25] P. Jansook, N. Ogawa, T. Loftsson, Cyclodextrins: structure, physicochemical properties and pharmaceutical applications, *International Journal of Pharmaceutics*. 535 (2018) 272–284. <https://doi.org/10.1016/j.ijpharm.2017.11.018>.
- [26] H. Dodziuk, *Cyclodextrins and their complexes: chemistry, analytical methods, applications*, Wiley-VCH, Weinheim, 2006.
- [27] A. Gu, N.J. Wheate, Macrocycles as drug-enhancing excipients in pharmaceutical formulations, *J Incl Phenom Macrocycl Chem*. 100 (2021) 55–69. <https://doi.org/10.1007/s10847-021-01055-9>.
- [28] R.L. Carrier, L.A. Miller, I. Ahmed, The utility of cyclodextrins for enhancing oral bioavailability, *Journal of Controlled Release*. 123 (2007) 78–99. <https://doi.org/10.1016/j.jconrel.2007.07.018>.
- [29] P.J. Skrdla, P.D. Floyd, P.C. Dell’orco, Practical Estimation of Amorphous Solubility Enhancement Using Thermoanalytical Data: Determination of the Amorphous/Crystalline Solubility Ratio for Pure Indomethacin and Felodipine, *Journal of Pharmaceutical Sciences*. 105 (2016) 2625–2630. <https://doi.org/10.1016/j.xphs.2016.03.036>.
- [30] K.A. Graeser, J.E. Patterson, J.A. Zeitler, K.C. Gordon, T. Rades, Correlating thermodynamic and kinetic parameters with amorphous stability, *European Journal of Pharmaceutical Sciences*. 37 (2009) 492–498. <https://doi.org/10.1016/j.ejps.2009.04.005>.
- [31] B.C. Hancock, G. Zografi, Characteristics and Significance of the Amorphous State in Pharmaceutical Systems, *Journal of Pharmaceutical Sciences*. 86 (1997) 1–12. <https://doi.org/10.1021/js9601896>.
- [32] T. Loftsson, M.E. Brewster, Pharmaceutical Applications of Cyclodextrins. 1. Drug Solubilization and Stabilization, *Journal of Pharmaceutical Sciences*. 85 (1996) 1017–1025. <https://doi.org/10.1021/js950534b>.
- [33] J. Kang, V. Kumar, D. Yang, P.R. Chowdhury, R.J. Hohl, Cyclodextrin complexation: influence on the solubility, stability, and cytotoxicity of camptothecin, an antineoplastic agent, *European Journal of Pharmaceutical Sciences*. 15 (2002) 163–170. [https://doi.org/10.1016/S0928-0987\(01\)00214-7](https://doi.org/10.1016/S0928-0987(01)00214-7).

- [34] A. Popielec, E. Fenyvesi, K. Yannakopoulou, T. Loftsson, Effect of cyclodextrins on the degradation rate of benzylpenicillin, *Pharmazie*. (2016) 68–75. <https://doi.org/10.1691/ph.2016.5114>.
- [35] C. Garnero, V. Aiassa, M. Longhi, Sulfamethoxazole:hydroxypropyl- β -cyclodextrin complex: preparation and characterization, *Journal of Pharmaceutical and Biomedical Analysis*. 63 (2012) 74–79. <https://doi.org/10.1016/j.jpba.2012.01.011>.
- [36] C. Fernandes, I. Encarnação, A. Gaspar, J. Garrido, F. Borges, E.M. Garrido, Influence of Hydroxypropyl- β -Cyclodextrin on the Photostability of Fungicide Pyrimethanil, *International Journal of Photoenergy*. 2014 (2014) 1–8. <https://doi.org/10.1155/2014/489873>.
- [37] I.A. Alsarra, M.O. Ahmed, M. El-Badry, F.K. Alanazi, A.M. Al-Mohizea, S.M. Ahmed, Effect of β -cyclodextrin derivatives on the kinetics of degradation of cefotaxime sodium in solution state, *Journal of Drug Delivery Science and Technology*. 17 (2007) 353–357. [https://doi.org/10.1016/S1773-2247\(07\)50054-7](https://doi.org/10.1016/S1773-2247(07)50054-7).
- [38] J. Hong, J.C. Shah, M.D. Mcgonagle, Effect of Cyclodextrin Derivation and Amorphous State of Complex on Accelerated Degradation of Ziprasidone, *Journal of Pharmaceutical Sciences*. 100 (2011) 2703–2716. <https://doi.org/10.1002/jps.22498>.
- [39] A. Popielec, T. Loftsson, Effects of cyclodextrins on the chemical stability of drugs, *International Journal of Pharmaceutics*. 531 (2017) 532–542. <https://doi.org/10.1016/j.ijpharm.2017.06.009>.
- [40] M. Di Cagno, The Potential of Cyclodextrins as Novel Active Pharmaceutical Ingredients: A Short Overview, *Molecules*. 22 (2016) 1. <https://doi.org/10.3390/molecules22010001>.
- [41] P. Mura, Analytical techniques for characterization of cyclodextrin complexes in the solid state: A review, *Journal of Pharmaceutical and Biomedical Analysis*. 113 (2015) 226–238. <https://doi.org/10.1016/j.jpba.2015.01.058>.
- [42] S. Kumar, R. Rao, Analytical tools for cyclodextrin nanosponges in pharmaceutical field: a review, *J Incl Phenom Macrocycl Chem*. 94 (2019) 11–30. <https://doi.org/10.1007/s10847-019-00903-z>.
- [43] J. Jablan, G. Szalontai, M. Jug, Comparative analysis of zaleplon complexation with cyclodextrins and hydrophilic polymers in solution and in solid state, *Journal of Pharmaceutical and Biomedical Analysis*. 71 (2012) 35–44. <https://doi.org/10.1016/j.jpba.2012.07.027>.
- [44] N. Mennini, M. Bragagni, F. Maestrelli, P. Mura, Physico-chemical characterization in solution and in the solid state of clonazepam complexes with native and chemically-modified cyclodextrins, *Journal of Pharmaceutical and Biomedical Analysis*. 89 (2014) 142–149. <https://doi.org/10.1016/j.jpba.2013.11.009>.
- [45] M. Jug, I. Kosalec, F. Maestrelli, P. Mura, Analysis of triclosan inclusion complexes with β -cyclodextrin and its water-soluble polymeric derivative, *Journal of Pharmaceutical and Biomedical Analysis*. 54 (2011) 1030–1039. <https://doi.org/10.1016/j.jpba.2010.12.009>.
- [46] M. Jug, N. Mennini, K.E. Kövér, P. Mura, Comparative analysis of binary and ternary cyclodextrin complexes with econazole nitrate in solution and in solid state, *Journal of Pharmaceutical and Biomedical Analysis*. 91 (2014) 81–91. <https://doi.org/10.1016/j.jpba.2013.12.029>.
- [47] Z. Aigner, O. Berkesi, G. Farkas, P. Szabó-Révész, DSC, X-ray and FTIR studies of a gemfibrozil/dimethyl- β -cyclodextrin inclusion complex produced by co-grinding, *Journal of Pharmaceutical and Biomedical Analysis*. 57 (2012) 62–67. <https://doi.org/10.1016/j.jpba.2011.08.034>.
- [48] G. Corti, G. Capasso, F. Maestrelli, M. Cirri, P. Mura, Physical–chemical characterization of binary systems of metformin hydrochloride with triacetyl- β -cyclodextrin, *Journal of Pharmaceutical and Biomedical Analysis*. 45 (2007) 480–486. <https://doi.org/10.1016/j.jpba.2007.07.018>.
- [49] M. Cirri, F. Maestrelli, S. Furlanetto, P. Mura, Solid-state characterization of glyburide-cyclodextrin co-ground products, *Journal of Thermal Analysis and Calorimetry*. 77 (2004) 413–422. <https://doi.org/10.1023/B:JTAN.0000038982.40315.8f>.

- [50] M. Jug, F. Maestrelli, M. Bragagni, P. Mura, Preparation and solid-state characterization of bupivacaine hydrochloride cyclodextrin complexes aimed for buccal delivery, *Journal of Pharmaceutical and Biomedical Analysis*. 52 (2010) 9–18. <https://doi.org/10.1016/j.jpba.2009.11.013>.
- [51] E. Redenti, L. Szente, J. Szejtli, Drug/Cyclodextrin/Hydroxy Acid Multicomponent Systems. Properties and Pharmaceutical Applications, *Journal of Pharmaceutical Sciences*. 89 (2000) 1–8. [https://doi.org/10.1002/\(SICI\)1520-6017\(200001\)89:1<1::AID-JPS1>3.0.CO;2-W](https://doi.org/10.1002/(SICI)1520-6017(200001)89:1<1::AID-JPS1>3.0.CO;2-W).
- [52] V. Aiassa, C. Garnero, M.R. Longhi, A. Zoppi, Cyclodextrin Multicomponent Complexes: Pharmaceutical Applications, *Pharmaceutics*. 13 (2021) 1099. <https://doi.org/10.3390/pharmaceutics13071099>.
- [53] T. Loftsson, M.E. Brewster, Cyclodextrins as Functional Excipients: Methods to Enhance Complexation Efficiency, *Journal of Pharmaceutical Sciences*. 101 (2012) 3019–3032. <https://doi.org/10.1002/jps.23077>.
- [54] H. Arima, K. Motoyama, T. Irie, Recent Findings on Safety Profiles of Cyclodextrins, Cyclodextrin Conjugates, and Polypseudorotaxanes, in: E. Bilensoy (Ed.), *Cyclodextrins in Pharmaceutics, Cosmetics, and Biomedicine*, John Wiley & Sons, Inc., Hoboken, NJ, USA, 2011: pp. 91–122. <https://doi.org/10.1002/9780470926819.ch5>.
- [55] E. Redenti, L. Szente, J. Szejtli, Cyclodextrin complexes of salts of acidic drugs. Thermodynamic properties, structural features, and pharmaceutical applications, *Journal of Pharmaceutical Sciences*. 90 (2001) 979–986. <https://doi.org/10.1002/jps.1050>.
- [56] T. Loftsson, M. Masson, The effects of water-soluble polymers on cyclodextrins and cyclodextrin solubilization of drugs, *Journal of Drug Delivery Science and Technology*. 14 (2004) 35–43. [https://doi.org/10.1016/S1773-2247\(04\)50003-5](https://doi.org/10.1016/S1773-2247(04)50003-5).
- [57] A.R. Tekade, J.N. Yadav, A Review on Solid Dispersion and Carriers Used Therein for Solubility Enhancement of Poorly Water Soluble Drugs, *Adv Pharm Bull*. 10 (2020) 359–369. <https://doi.org/10.34172/apb.2020.044>.
- [58] P. Saokham, C. Muangkaew, P. Jansook, T. Loftsson, Solubility of Cyclodextrins and Drug/Cyclodextrin Complexes, *Molecules*. 23 (2018) 1161. <https://doi.org/10.3390/molecules23051161>.
- [59] P. Suvarna, P. Chaudhari, S.A. Lewis, Cyclodextrin-Based Supramolecular Ternary Complexes: Emerging Role of Ternary Agents on Drug Solubility, Stability, and Bioavailability, *Crit Rev Ther Drug Carrier Syst*. 39 (2022) 1–50. <https://doi.org/10.1615/CritRevTherDrugCarrierSyst.2022038870>.
- [60] S. Jacob, A.B. Nair, Cyclodextrin complexes: Perspective from drug delivery and formulation, *Drug Dev Res*. 79 (2018) 201–217. <https://doi.org/10.1002/ddr.21452>.
- [61] E.M.M. Del Valle, Cyclodextrins and their uses: a review, *Process Biochemistry*. 39 (2004) 1033–1046. [https://doi.org/10.1016/S0032-9592\(03\)00258-9](https://doi.org/10.1016/S0032-9592(03)00258-9).
- [62] L.A. Miller, R.L. Carrier, I. Ahmed, Practical considerations in development of solid dosage forms that contain cyclodextrin, *Journal of Pharmaceutical Sciences*. 96 (2007) 1691–1707. <https://doi.org/10.1002/jps.20831>.
- [63] G. Wypych, *Handbook of Solvents*, Third, 2019.
- [64] V. Martinez, T. Stolar, B. Karadeniz, I. Brekalo, K. Užarević, Advancing mechanochemical synthesis by combining milling with different energy sources, *Nat Rev Chem*. 7 (2022) 51–65. <https://doi.org/10.1038/s41570-022-00442-1>.
- [65] I. Colombo, G. Grassi, M. Grassi, Drug mechanochemical activation, *Journal of Pharmaceutical Sciences*. 98 (2009) 3961–3986. <https://doi.org/10.1002/jps.21733>.

- [66] M. Jug, P. Mura, Grinding as Solvent-Free Green Chemistry Approach for Cyclodextrin Inclusion Complex Preparation in the Solid State, *Pharmaceutics*. 10 (2018) 189. <https://doi.org/10.3390/pharmaceutics10040189>.
- [67] D.N. Bikiaris, Solid dispersions, Part I: recent evolutions and future opportunities in manufacturing methods for dissolution rate enhancement of poorly water-soluble drugs, *Expert Opinion on Drug Delivery*. 8 (2011) 1501–1519. <https://doi.org/10.1517/17425247.2011.618181>.
- [68] D. He, P. Deng, L. Yang, Q. Tan, J. Liu, M. Yang, J. Zhang, Molecular encapsulation of rifampicin as an inclusion complex of hydroxypropyl- β -cyclodextrin: Design; characterization and in vitro dissolution, *Colloids and Surfaces B: Biointerfaces*. 103 (2013) 580–585. <https://doi.org/10.1016/j.colsurfb.2012.10.062>.
- [69] J.L. Howard, Q. Cao, D.L. Browne, Mechanochemistry as an emerging tool for molecular synthesis: what can it offer?, *Chem. Sci*. 9 (2018) 3080–3094. <https://doi.org/10.1039/C7SC05371A>.
- [70] H.R.H. Ali, I.Y. Saleem, H.M. Tawfeek, Insight into inclusion complexation of indomethacin nicotinamide cocrystals, *J Incl Phenom Macrocycl Chem*. 84 (2016) 179–188. <https://doi.org/10.1007/s10847-016-0594-3>.
- [71] M. Brusnikina, O. Silyukov, M. Chislov, T. Volkova, A. Proshin, A. Mazur, P. Tolstoy, I. Terekhova, Effect of cyclodextrin complexation on solubility of novel anti-Alzheimer 1,2,4-thiadiazole derivative, *J Therm Anal Calorim*. 130 (2017) 443–450. <https://doi.org/10.1007/s10973-017-6252-1>.
- [72] S. Li, X. Lin, K. Xu, J. He, H. Yang, H. Li, Co-grinding Effect on Crystalline Zaltoprofen with β -cyclodextrin/Cucurbit[7]uril in Tablet Formulation, *Sci Rep*. 7 (2017) 45984. <https://doi.org/10.1038/srep45984>.
- [73] M. Leonardi, M. Villacampa, J.C. Menéndez, Multicomponent mechanochemical synthesis, *Chem. Sci*. 9 (2018) 2042–2064. <https://doi.org/10.1039/C7SC05370C>.
- [74] S. Stegemann, I. Klebovich, I. Antal, H.H. Blume, K. Magyar, G. Németh, T.L. Paál, W. Stumptner, G. Thaler, A. Van de Putte, V.P. Shah, Improved therapeutic entities derived from known generics as an unexplored source of innovative drug products, *European Journal of Pharmaceutical Sciences*. 44 (2011) 447–454. <https://doi.org/10.1016/j.ejps.2011.09.012>.
- [75] Cision PR Newswire, (2022). <https://www.prnewswire.co.uk/news-releases/drug-delivery-systems-market-size-worth-us-363-82-billion-with-cagr-of-6-10-from-2022-to-2030--exclusive-report-by-growth-plus-reports-301637706.html> (accessed 3 May 2023).
- [76] J. Rincón-López, Y.C. Almanza-Arjona, A.P. Riascos, Y. Rojas-Aguirre, Technological evolution of cyclodextrins in the pharmaceutical field, *Journal of Drug Delivery Science and Technology*. 61 (2021) 102156. <https://doi.org/10.1016/j.jddst.2020.102156>.
- [77] T. Loftsson, D. Duchene, Cyclodextrins and their pharmaceutical applications, *International Journal of Pharmaceutics*. (2007) 11.
- [78] N. Morin-Crini, S. Fourmentin, É. Fenyvesi, E. Lichtfouse, G. Torri, M. Fourmentin, G. Crini, 130 years of cyclodextrin discovery for health, food, agriculture, and the industry: a review, *Environ Chem Lett*. 19 (2021) 2581–2617. <https://doi.org/10.1007/s10311-020-01156-w>.
- [79] I. Puskás, L. Szente, L. Szócs, É. Fenyvesi, Recent List of Cyclodextrin-Containing Drug Products, *Period. Polytech. Chem. Eng*. 67 (2023) 11–17. <https://doi.org/10.3311/PPch.21222>.
- [80] J. Leyden, Pharmacokinetics and pharmacology of terbinafine and itraconazole, *Journal of the American Academy of Dermatology*. 38 (1998) S42–S47. [https://doi.org/10.1016/S0190-9622\(98\)70483-9](https://doi.org/10.1016/S0190-9622(98)70483-9).
- [81] N.H. Shear, V.V. Villars, C. Marsolais, Terbinafine: An oral and topical antifungal agent, *Clinics in Dermatology*. 9 (1991) 487–495. [https://doi.org/10.1016/0738-081X\(91\)90077-X](https://doi.org/10.1016/0738-081X(91)90077-X).

- [82] J.A. Balfour, D. Faulds, Terbinafine: A Review of its Pharmacodynamic and Pharmacokinetic Properties, and Therapeutic Potential in Superficial Mycoses, *Drugs*. 43 (1992) 259–284. <https://doi.org/10.2165/00003495-199243020-00010>.
- [83] J.G.V.D. Schroeffer, P.K.S. Cirkel, M.B. Crijns, T.J.A.V. Dijk, F.J. Govaert, D.A. Groeneweg, D.J. Tazelaar, R.F.E.D. Wit, J. Wuite, A randomized treatment duration-finding study of terbinafine in onychomycosis, *Br J Dermatol*. 126 (1992) 36–39. <https://doi.org/10.1111/j.1365-2133.1992.tb00008.x>.
- [84] B.H.Ch. Stricker, M.M. Van Riemsdijk, M.C.J.M. Sturkenboom, J.P. Ottervanger, Taste loss to terbinafine: a case-control study of potential risk factors, *British Journal of Clinical Pharmacology*. 42 (1996) 313–318. <https://doi.org/10.1046/j.1365-2125.1996.04105.x>.
- [85] Gupta, Lynde, Lauzon, Mehlmauer, Braddock, Miller, Del Rosso, Shear, Cutaneous adverse effects associated with terbinafine therapy: 10 case reports and a review of the literature, *British Journal of Dermatology*. 138 (1998) 529–532. <https://doi.org/10.1046/j.1365-2133.1998.02140.x>.
- [86] C. Ajit, N. Zaeri, S.J. Munoz, A. Suvannasankha, Terbinafine-Associated Hepatotoxicity, *The American Journal of the Medical Sciences*. 325 (2003) 292–295. <https://doi.org/10.1097/00000441-200305000-00008>.
- [87] P. Chouhan, T.R. Saini, Hydroxypropyl- β -cyclodextrin: A Novel Transungual Permeation Enhancer for Development of Topical Drug Delivery System for Onychomycosis, *Journal of Drug Delivery*. 2014 (2014) 1–7. <https://doi.org/10.1155/2014/950358>.
- [88] M. Uzqueda, C. Martín, A. Zornoza, M. Sánchez, I. Vélaz, Physicochemical characterization of terbinafine-cyclodextrin complexes in solution and in the solid state, *J Incl Phenom Macrocycl Chem*. 66 (2010) 393–402. <https://doi.org/10.1007/s10847-009-9656-0>.
- [89] B. Staels, J. Dallongeville, J. Auwerx, K. Schoonjans, E. Leitersdorf, J.-C. Fruchart, Mechanism of Action of Fibrates on Lipid and Lipoprotein Metabolism, *Circulation*. 98 (1998) 2088–2093. <https://doi.org/10.1161/01.CIR.98.19.2088>.
- [90] J.A. Balfour, D. McTavish, R.C. Heel, Fenofibrate: A Review of its Pharmacodynamic and Pharmacokinetic Properties and Therapeutic Use in Dyslipidaemia, *Drugs*. 40 (1990) 260–290. <https://doi.org/10.2165/00003495-199040020-00007>.
- [91] D.R.P. Guay, Update on Fenofibrate, *Cardiovascular Drug Reviews*. 20 (2006) 281–302. <https://doi.org/10.1111/j.1527-3466.2002.tb00098.x>.
- [92] T.N. Nguyen, J.-S. Park, Exploring Fenofibrate Formulations for the Treatment of Lipid Disorders: Past, Present, and Future, *Cardiometab Syndr J*. 2 (2022) 77. <https://doi.org/10.51789/cmsj.2022.2.e13>.
- [93] P. Tipduangta, K. Takieddin, L. Fábíán, P. Belton, S. Qi, A New Low Melting-Point Polymorph of Fenofibrate Prepared via Talc Induced Heterogeneous Nucleation, *Crystal Growth & Design*. 15 (2015) 5011–5020. <https://doi.org/10.1021/acs.cgd.5b00956>.
- [94] M. Vogt, K. Kunath, J.B. Dressman, Dissolution enhancement of fenofibrate by micronization, cogrinding and spray-drying: Comparison with commercial preparations, *European Journal of Pharmaceutics and Biopharmaceutics*. 68 (2008) 283–288. <https://doi.org/10.1016/j.ejpb.2007.05.010>.
- [95] R. Kumar, Solubility and Bioavailability of Fenofibrate Nanoformulations, *ChemistrySelect*. 5 (2020) 1478–1490. <https://doi.org/10.1002/slct.201903647>.
- [96] S.K. Jagdale, M.H. Dehghan, N.S. Paul, Enhancement of Dissolution of Fenofibrate Using Complexation with Hydroxy Propyl β -Cyclodextrin, *Tjps*. 16 (2019) 48–53. <https://doi.org/10.4274/tjps.60490>.
- [97] S.Y. Khin, H.M.S.H. Soe, C. Chansrinoyom, N. Pornputtapong, R. Asasutjarit, T. Loftsson, P. Jansook, Development of Fenofibrate/Randomly Methylated β -Cyclodextrin-Loaded Eudragit®

- RL 100 Nanoparticles for Ocular Delivery, *Molecules*. 27 (2022) 4755.
<https://doi.org/10.3390/molecules27154755>.
- [98] Z. Aigner, I. Bencz, M. Kata, Increasing the solubility characteristics of fenofibrate with cyclodextrin, *J Incl Phenom Macrocycl Chem*. 20 (1995) 241–252.
<https://doi.org/10.1007/BF00708770>.
- [99] T. Loftsson, H.H. Sigurdsson, P. Jansook, Anomalous Properties of Cyclodextrins and Their Complexes in Aqueous Solutions, *Materials*. 16 (2023) 2223.
<https://doi.org/10.3390/ma16062223>.
- [100] T. Loftsson, M.E. Brewster, Pharmaceutical applications of cyclodextrins: basic science and product development, *Journal of Pharmacy and Pharmacology*. 62 (2010) 1607–1621.
<https://doi.org/10.1111/j.2042-7158.2010.01030.x>.
- [101] V.J. Stella, Q. He, Cyclodextrins, *Toxicol Pathol*. 36 (2008) 30–42.
<https://doi.org/10.1177/0192623307310945>.
- [102] F. Menges, Spectragryph - optical spectroscopy software, (2022).
<https://www.ffmpeg2.de/spectragryph/>.
- [103] M. Rams-Baron, R. Jachowicz, E. Boldyreva, D. Zhou, W. Jamroz, M. Paluch, Physical Instability: A Key Problem of Amorphous Drugs, in: *Amorphous Drugs*, Springer International Publishing, Cham, 2018: pp. 107–157. https://doi.org/10.1007/978-3-319-72002-9_5.

ACKNOWLEDGEMENTS

This work was supported by ÚNKP-22-3 New National Excellence Program of the Ministry for Innovation and Technology from the source of The National Research Development and Innovation Fund, the Gedeon Richter's Centenary Foundation (Budapest).

I would like to thank **Prof. Dr. Ildikó Csóka** my supervisor and head of the Institute of Pharmaceutical Technology and Regulatory Affairs for providing me the high-quality conditions to work as Ph.D. student.

Many thanks to my former supervisor **Dr. habil Zoltán Aigner, Ph.D.**, who introduced me to my research topic as a graduate student. It was with his guidance that I started my Ph.D. work, for which I will never be able to truly thank him.

I am grateful to my supervisor, **Dr. habil Rita Ambrus Ph.D.** giving me her endless support and expert guidance during my Ph.D. studies, which has helped me to develop my skills, both professionally and as a person. Among the co-authors, I would like to thank **Dr. Orsolya Jójárt-Laczkovich Ph.D.** and **Dr.habil Ottó Berkesi Ph.D.** for the help. I would like to thank the staff of the institute for their help, especially **Klára Kovács**, who, in addition to being a great help in the lab, was always eager to help me achieve my goals from the beginning of my scientific work.

I owe many thanks to **my family, friends** and **partner, Dr. Ibolya Tóth** for their endless encouragement and loving support towards me.